Cellular/Molecular

mGluR5 from Primary Sensory Neurons Promotes Opioid-Induced Hyperalgesia and Tolerance by Interacting with and Potentiating Synaptic NMDA Receptors

Daozhong Jin (金道忠), Hong Chen (陈红), Meng-Hua Zhou (周孟华), Shao-Rui Chen (陈少瑞), and Hui-Lin Pan (潘惠麟)

Center for Neuroscience and Pain Research, Department of Anesthesiology and Perioperative Medicine, University of Texas MD Anderson Cancer Center, Houston, Texas 77030

Aberrant activation of presynaptic NMDARs in the spinal dorsal horn is integral to opioid-induced hyperalgesia and analgesic tolerance. However, the signaling mechanisms responsible for opioid-induced NMDAR hyperactivity remain poorly identified. Here, we show that repeated treatment with morphine or fentanyl reduced monomeric mGluR5 protein levels in the dorsal root ganglion (DRG) but increased levels of mGluR5 monomers and homodimers in the spinal cord in mice and rats of both sexes. Coimmunoprecipitation analysis revealed that monomeric and dimeric mGluR5 in the spinal cord, but not monomeric mGluR5 in the DRG, directly interacted with GluN1. By contrast, mGluR5 did not interact with μ-opioid receptors in the DRG or spinal cord. Repeated morphine treatment markedly increased the mGluR5-GluN1 interaction and protein levels of mGluR5 and GluN1 in spinal synaptosomes. The mGluR5 antagonist MPEP reversed morphine treatment-augmented mGluR5-GluN1 interactions, GluN1 synaptic expression, and dorsal root-evoked monosynaptic EPSCs of dorsal horn neurons. Furthermore, CRISPR-Cas9–induced conditional mGluR5 knockdown in DRG neurons normalized mGluR5 levels in spinal synaptosomes and NMDAR-mediated EPSCs of dorsal horn neurons increased by morphine treatment. Correspondingly, intrathecal injection of MPEP or conditional mGluR5 knockdown in DRG neurons not only potentiated the acute analgesic effect of morphine but also attenuated morphine treatment-induced hyperalgesia and tolerance. Together, our findings suggest that opioid treatment promotes mGluR5 trafficking from primary sensory neurons to the spinal dorsal horn. Through dimerization and direct interaction with NMDARs, presynaptic mGluR5 potentiates and/or stabilizes NMDAR synaptic expression and activity at primary afferent central terminals, thereby maintaining opioid-induced hyperalgesia and tolerance.

Key words: Grm5; **metabotropic glutamate receptor 5; μ-opioid receptor; *N*-methyl-*D*-aspartate receptor; protein oligomerization; synaptic plasticity**

Significance Statement

Opioids are essential analgesics for managing severe pain caused by cancer, surgery, and tissue injury. However, these drugs paradoxically induce pain hypersensitivity and tolerance, which can cause rapid dose escalation and even overdose mortality. This study demonstrates, for the first time, that opioids promote trafficking of mGluR5, a G protein-coupled glutamate receptor, from peripheral sensory neurons to the spinal cord; there, mGluR5 proteins dimerize and physically interact with NMDARs to augment their synaptic expression and activity. Through dynamic interactions, the two distinct glutamate receptors mutually amplify and sustain nociceptive input from peripheral sensory neurons to the spinal cord. Thus, inhibiting mGluR5 activity or disrupting mGluR5–NMDAR interactions could reduce opioid-induced hyperalgesia and tolerance and potentiate opioid analgesic efficacy.

Received Mar. 31, 2023; revised June 29, 2023; accepted July 4, 2023.

Author contributions: D.J., H.C., M.-H.Z., and S.-R.C. performed research; D.J., H.C., M.-H.Z., S.-R.C., and H.-L.P. analyzed data; D.J. wrote the first draft of the paper; S.-R.C. and H.-L.P. designed research; S.-R.C. and H.-L.P. edited the paper.

This work was supported by National Institutes of Health Grants DA041711 and NS101880; and by the Pamela and Wayne Garrison Distinguished Chair Endowment. We thank Amy Ninetto (MD Anderson Cancer Center) for proofreading the manuscript.

The authors declare no competing financial interests.

Correspondence should be addressed to Hui-Lin Pan at huilinpan@mdanderson.org or Shao-Rui Chen at schen@mdanderson.org.

https://doi.org/10.1523/JNEUROSCI.0601-23.2023

Introduction

The μ-opioid receptor (MOR) agonists are the first-line treatment for severe pain caused by cancer, surgery, and tissue injury. Paradoxically, however, prolonged opioid use produces hyperalgesia and analgesic tolerance, causing rapid dose escalation of opioids and potentially resulting in dependence, addiction, and even overdose death. Recent evidence using conditional MOR knockout (KO) mice indicates that MORs expressed in primary sensory neurons and their afferent terminals in the spinal cord play an essential role in both opioid-elicited synaptic LTP as well as opioid-induced analgesia and hyperalgesia (Sun et al., 2019; S.

R. Chen et al., 2022). Also, brief and repeated treatment with MOR agonists potentiates presynaptic NMDAR activity in the spinal dorsal horn, which plays a prominent role in the development of opioid-induced hyperalgesia and tolerance (H. Y. Zhou et al., 2010; Zhao et al., 2012; Deng et al., 2019a; S. R. Chen et al., 2022). However, exactly how MOR activation leads to increased presynaptic NMDAR activity in the spinal cord is largely unknown. The C-terminal domains of NMDAR subunits can be phosphorylated by various protein kinases, including PKC (Sprengel et al., 1998; M. H. Zhou et al., 2021b). In this regard, phosphorylation of NMDARs by PKC regulates NMDAR activity and associated synaptic plasticity in the spinal cord (M. H. Zhou et al., 2021b; S. R. Chen et al., 2022). Inhibition of PKC or Gαq/11 at the spinal cord level augments opioids' analgesic effect and reduces opioid-induced NMDAR hyperactivity and hyperalgesia (Zhao et al., 2012; S. R. Chen et al., 2022; Marwari et al., 2022). Because MORs are typically coupled to inhibitory Gαi/o proteins, it remains difficult to understand how MOR agonists induce activation of Gαq/11 and PKC in the spinal cord.

mGluR5 (meabotropic glutamate receptor 5, encoded by the *Grm5* gene), one member of Group I mGluRs that are coupled to Gαq/11, is broadly expressed in peripheral and central neurons, including those of the DRG and spinal cord (Alvarez et al., 2000; Hudson et al., 2002; Xie et al., 2017). Increased mGluR5 activity can augment nociceptive transmission at the spinal cord level. For instance, intrathecal administration of the mGluR5 antagonist MPEP ameliorates neuropathic pain in animal models (Sotgiu et al., 2003; J. Q. Li et al., 2010; Xie et al., 2017). Upon activation, mGluR5 stimulates PLC via coupling to stimulatory Gαq/11 proteins to hydrolyze phosphoinositides (Conn and Pin, 1997; Miura et al., 2002). Hydrolyzation of phosphoinositides produces diacylglycerol, an activator of PKC, and inositol-1,4,5-triphosphate, which releases Ca^{2+} from internal stores (Abdul-Ghani et al., 1996). This stimulatory activity gives mGluR5 a potential role in opioid-induced NMDAR hyperactivity via PKC. Indeed, constitutive mGluR5 KO in mice (M. Huang et al., 2019) or intrathecal injection of MPEP (Xu et al., 2007; Liu et al., 2009) attenuates morphine-induced hyperalgesia and tolerance. Also, repeated morphine treatment increases mGluR5 and GluN1 expression in the spinal cord (Narita et al., 2005; Liu et al., 2009). Prior activation of mGluR5 converts the action of Gαi/o-coupled Group III mGluRs from inhibitory to excitatory in neurons (J. J. Zhou et al., 2020). Thus, activation of PKC by the Gαq/11-coupled mGluR5 provides an opportunity to augment and/or maintain opioid-induced phosphorylation and activation of NMDARs. However, the interplay between mGluR5 and NMDARs in opioid-induced hyperalgesia and tolerance is poorly understood.

In the present study, we determined the potential role of mGluR5 from DRG neurons in opioid-induced presynaptic NMDAR hyperactivity in the spinal cord. We showed, for the first time, that repeated opioid treatment promotes mGluR5 trafficking from the DRG to spinal cord. In the spinal cord, mGluR5 forms homodimers and interacts with NMDARs to augment and/or maintain synaptic expression and activity of NMDARs. Importantly, our study reveals that mGluR5 from DRG neurons mediates opioid-induced hyperalgesia and tolerance by promoting NMDAR-mediated glutamatergic input to the spinal dorsal horn. This new information advances our understanding of the signaling mechanism responsible for opioid-induced hyperalgesia and tolerance.

Materials and Methods

Animals. The Institutional Animal Care and Use Committee of the University of Texas MD Anderson Cancer Center approved all experimental procedures and protocols. The *Guide for the care and use of laboratory animals* (National Institutes of Health) was followed throughout the study. Adult male and female Sprague Dawley rats (180-250 g) were used in this study and housed with no more than 3 rats per cage. $Cas9^{Flox/+}$ mice were purchased from The Jackson Laboratory (stock #026175). Advillin-Cre ($Avil^{Cre/+}$) mice (da Silva et al., 2011) were kindly provided by Fan Wang (Massachusetts Institute of Technology). We bred $Cas9^{Flox/+}$ female and male mice to obtain $Cas9^{Flox/Flox}$ mice. To induce Cas9 "knock-in" in primary sensory neurons, $Avil^{Cre/+}$::$Cas9^{Flox/+}$ mice were obtained by breeding the male $Avil^{Cre/+}$ mice with female $Cas9^{Flox/Flox}$ mice. Because $Cas9^{Flox/+}$ mice have a floxed-STOP cassette preventing expression of Cas9, Cas9 is expressed only after exposure to the Cre recombinase. Mice were earmarked 3 weeks after birth, and ear biopsies were used to confirm the genotype. All the mice had a C57BL/6 genetic background and were housed with no more than 5 mice per cage. Adult male and female mice (8-12 weeks old) were used for final experiments.

For induction of opioid-induced hyperalgesia and tolerance, we intraperitoneally injected mice (10 mg/kg, twice per day) and rats (5 mg/kg, twice per day) with morphine (catalog #0641-6127-25, West Ward Pharmaceuticals) for 8 and 7 consecutive days for mice and rats, respectively (S. R. Chen et al., 2007; Zhao et al., 2012; Jin et al., 2022). Some mice were also treated with fentanyl (0.1 mg/kg, i.p., twice per day, catalog #0641-6028-01, West Ward Pharmaceuticals) for 8 consecutive days (Sun et al., 2019).

Construction of lentiviral vectors expressing mGluR5-specific guide RNA (gRNA). We constructed a lentivirus that expresses a gRNA against mouse mGluR5 (encoded by the *Grm5* gene) using previously described methods (Sanjana et al., 2014; Shalem et al., 2014). Briefly, we first cloned four specific gRNAs against *Grm5* into a lentiGuide-Puro plasmid (catalog #52963, Addgene). To determine the effect of the gRNA-containing lentiGuide-Puro plasmids on mGluR5 knockdown, we cloned the full-length *Grm5* coding sequence into a pcDNA6 plasmid. The gRNA-containing lentiGuide-Puro plasmids were cotransfected with pcDNA6-*Grm5* and lentiCas9 plasmids (catalog #63592, Addgene) into HEK293FT cells using Polyjet transfection reagent (catalog #SL100688, SignaGen Laboratories). After 3 d of coincubation, the cells were collected for immunoblot analysis to confirm mGluR5 knockdown. The most effective lentiGuide-Puro plasmid for mGluR5 knockdown was then packaged into the lentivirus through cotransfecting with the packaging plasmids pCMV-VSV-G (catalog #8454, Addgene) and psPAX2 (catalog #12260, Addgene) into HEK293FT cells. The virus-containing culture medium was collected after 72 h of culture. The virus was concentrated 100 times using a Lenti-X concentrator reagent (catalog #631231, Takara Bio), and the viral titer was determined using a titration reagent (catalog #VPK-112, Cell Biolabs). The concentrated virus with a titer of 4×10^{12} virus particles/ml was stored at −80°C until use. We used the pLJM1-EGFP plasmid (catalog #19319, Addgene) as a negative control to allow monitoring of successful transfection in HEK293FT cells and lentivirus preparation. The negative control virus was made using the pLJM1-EGFP plasmid on the same lentivirus-based backbone and was packaged similarly to the mGluR5 gRNA-containing virus.

Tissue collection, spinal synaptosome preparation, and coimmunoprecipitation. The mice and rats were decapitated after being anesthetized with 3% isoflurane. The DRGs and the dorsal spinal cord at lumbar L3-L5 levels were harvested for RNA and protein analyses. Total proteins of the DRG and dorsal spinal cord tissues used for immunoblotting were extracted using RIPA lysis buffer (catalog #20-188, Millipore-Sigma). To isolate the synaptosomal proteins of the spinal cord, the spinal cord tissues were homogenized in ice-cold homogenization buffer containing 0.32 M sucrose, 10 mM HEPES, 2 mM EDTA (pH, 7.4), and a protease inhibitor cocktail (catalog #P8340, Millipore-Sigma), as we described previously (J. Chen et al., 2018; Y. Huang et al., 2020). The homogenate was centrifuged at 800 × *g* for 10 min at 4°C to remove insoluble cell debris. The supernatant was then centrifuged at 13,000 × *g* for 20 min to obtain the crude synaptosomes. The synaptosome pellets for immunoblotting

were solubilized in RIPA lysis buffer with a protease inhibitor cocktail for 1 h on ice and then centrifuged at 10,000 × *g* for 15 min at 4°C. The total proteins and spinal cord synaptosomes used for immunoprecipitation were solubilized in immunoprecipitation lysis buffer containing 25 mM Tris-HCl (pH 7.4), 150 mM NaCl, 1 mM EDTA, 1% NP-40, 5% glycerol (catalog #87788, Fisher Scientific), and a proteinase inhibitor cocktail.

For coimmunoprecipitation, proteins were incubated at 4°C overnight with protein G beads (catalog #16-266, Millipore-Sigma) and a rabbit anti-mGluR5 antibody (1:500, catalog #AB5675, Millipore-Sigma), rabbit anti-GluN1 antibody (1:500, catalog #G8913, Millipore-Sigma), rabbit anti-MOR antibody (1:500, catalog #AB1580-I, Millipore-Sigma), or normal rabbit IgG (catalog #12-371, Millipore-Sigma). All samples were washed 3 times with immunoprecipitation lysis buffer. The beads were then incubated with 1 × NuPage loading buffer (catalog #NP0008, Fisher Scientific) with additional 100 mM DTT (catalog #P2325, Fisher Scientific) and 1% SDS (catalog #71736, Millipore-Sigma) for 10 min and boiled for 5 min. The eluted proteins were used for further immunoblotting analysis.

Immunoblotting. Immunoblotting was performed as described previously (Y. Huang et al., 2020; Jin et al., 2022). Briefly, proteins were separated on 4%-12% SDS NuPage, Bis-Tris gels (catalog #NP0336BOX, Fisher Scientific) and transferred to PVDF membranes (catalog #IPVH00010, Millipore-Sigma). Membranes were incubated with primary antibodies overnight at 4°C. This was followed by incubation with HRP-conjugated secondary antibodies (1:5000, anti-rabbit IgG, catalog #7074; anti-mouse IgG, catalog #7076; Cell Signaling Technology) for 1 h at 22°C. To detect protein expression levels from coimmunoprecipitation samples, HRP-conjugated Trueblot secondary antibodies were used (1:5000, anti-rabbit IgG, catalog #18-8816-31; anti-mouse IgG, catalog #18-8817-31, Rockland Immunochemicals). The membranes were thoroughly washed after each antibody incubation. Immunoblots were developed with an enhanced chemiluminescence kit (catalog #34095, Fisher Scientific). The protein bands were visualized using an Odyssey Fc Imager (LI-COR Biosciences) and quantified with ImageJ software. The primary antibodies included rabbit anti-mGluR5 (1:2000, catalog #AB5675, Millipore-Sigma), rabbit anti-GluN1 (1:1000, catalog #G8913, Millipore-Sigma), rabbit anti-MOR (1:1000, catalog #RA10104, Neuromics), mouse anti-β-actin (1:10,000, catalog #3700, Cell Signaling Technology), mouse anti-PSD95 (1:10,000, catalog #MABN1190, Millipore-Sigma), mouse anti-$\alpha 2\delta$-1 (1:1000, catalog #SC-271697, Santa Cruz Biotechnology), and mouse anti-Cas9 (catalog #14697, Cell Signaling Technology). The specificity of anti-MOR, anti-GluN1, and anti-$\alpha 2\delta$-1 antibodies has been validated using KO mice (J. Chen et al., 2018; Sun et al., 2019; Y. Huang et al., 2020; G. F. Zhang et al., 2021). For protein quantification, the protein band intensity was normalized to that of PSD95 or β-actin on the same gel.

qPCR. Total RNAs were extracted from the DRG and dorsal spinal cord tissues with a Trizol reagent (catalog #15596026, Fisher Scientific) according to the manufacturer's instructions. cDNA was prepared with a RevertAid RT Reverse Transcription Kit (catalog #K1691, Fisher Scientific). Real-time PCR was performed using SYBR GreenER qPCR SuperMix Universal kit (catalog #01143681, Fisher Scientific) and a Quant Studio 7 Flex Real-Time PCR System (Applied Biosystems). The thermal cycling conditions used were as follows: 1 cycle at 95°C for 5 min, 40 cycles at 95°C for 15 s, 60°C for 15 s, and 72°C for 30 s. Primers specific for both mouse and rat *Grm5* (mouse sequence ID: NM_001081414.2; rat sequence ID: XM_032893267.1) were as follows: GGAGCACCACCCCAAACT CT (forward) and GTGGCTCACAACGATGAAGAAC (reverse). Primers for β-actin (mouse sequence ID: NM_007393.5; rat sequence ID: NM_031144.3) were TACGTAGCCATCCAGGCTGTG (forward) and CAGCTCATAGCTCTTCTCCAG (reverse). Results are presented as expression levels relative to controls after normalizing to β-actin using the comparative C_t method.

Nociceptive behavioral tests. To measure the tactile withdrawal threshold, animals were placed in individual plastic boxes on a mesh floor. A series of calibrated von Frey filaments was applied perpendicularly to the plantar surface of the hindpaw with sufficient force to bend the filaments for 6 s. A brisk paw withdrawal or flinching was considered a positive response. In the absence of a response, the filament of next greater force was applied. If a response occurred, the filament of next lower force was applied. Six consecutive responses from the first change were used to calculate the withdrawal threshold (in grams) using the "up-down" method (Chaplan et al., 1994; S. R. Chen et al., 2014a).

The nociceptive mechanical threshold in response to a noxious pressure stimulus was tested with a digital Randall-Selitto paw pressure device (catalog #2500, IITC Life Science) as described previously (Jin et al., 2022; J. Zhang et al., 2022). The device was used to gently hold the animal's hindpaw, and a constantly increasing force was applied via a pointed end to the midplantar glabrous surface of the hindpaw. When the animal displayed a withdrawal response, the device was immediately stopped, and the threshold was recorded.

To assess thermal nociception, we measured the hindpaw withdrawal latency using a thermal testing apparatus (catalog #390G, IITC Life Science), as we described previously (Jin et al., 2022; Y. Huang et al., 2023). Animals were placed on a glass surface maintained at 30°C and were acclimated to the device. A mobile radiant heat stimulus was applied to the plantar surface of the hindpaw until the animal lifted or licked the hindpaw. The time of hindpaw withdrawal was recorded by a timer as the thermal withdrawal latency.

Electrophysiological recordings in spinal cord slices. The animals were anesthetized with 3% isoflurane, and the lumbar spinal cords at the L4-L6 levels were quickly removed via laminectomy. The animals were then killed via inhalation of 5% isoflurane followed by rapid decapitation. The spinal cords were immediately put into 95% O_2 and 5% CO_2 presaturated ice-cold ACSF containing the following reagents (in mM): 25 glucose, 234 sucrose, 3.6 KCl, 26 $NaHCO_3$, 1.2 NaH_2PO_4, 2.5 $CaCl_2$, and 1.2 $MgCl_2$. The spinal cord tissue was then glued onto the stage of a vibratome and cut into 400-μm-thick transverse slices. The slices were incubated in Krebs solution containing the following (in mM): 11 glucose, 117 NaCl, 3.6 KCl, 25 $NaHCO_3$, 1.2 NaH_2PO_4, 2.5 $CaCl_2$, and 1.2 $MgCl_2$ (gassed with 95% O_2 and 5% CO_2) at 34°C for at least 1 h before recordings. We then placed the spinal cord slices in the recording chamber with continuous perfusion of oxygenated Krebs solution (3 ml/min) at 34°C.

We identified neurons in the lamina II outer zone using infrared illumination and differential interference contrast under a microscope. EPSCs from these neurons were recorded using a whole-cell voltage-clamp mode at the holding potential of −60 mV as we described previously (S. R. Chen et al., 2014a, 2022). A glass pipette electrode (4-7 MΩ) was filled with the internal solution containing the following (in mM): 135 K-gluconate, 5 KCl, 2 $MgCl_2$, 0.5 $CaCl_2$, 5 EGTA, 5 HEPES, 0.5 Na_2-GTP, 5 Mg-ATP, and 10 lidocaine N-ethyl bromide (QX314; 280-300 mOsm, pH 7.3). QX314 was included in the pipette recording solution to suppress postsynaptic neuronal firing. EPSCs were evoked by electrical stimulation (0.6 mA, 0.5 ms, and 0.1 Hz) of the dorsal root to elicit glutamate release from primary afferent nerves. Monosynaptic EPSCs of lamina II neurons were identified based on the constant latency and absence of conduction failure of evoked EPSCs in response to 20 Hz electrical stimulation (H. Y. Zhou et al., 2010; Y. Huang et al., 2022). To determine the paired-pulse ratio (PPR), we generated a pair of stimuli at 50 ms intervals to evoke EPSCs. The PPR was expressed as the ratio of the amplitude of the second synaptic response to the amplitude of the first synaptic response (Xie et al., 2016; Y. Huang et al., 2020).

All signals were recorded using an amplifier (MultiClamp700B; Molecular Devices), filtered at 1-2 kHz, and digitized at 10 kHz. AP5 was purchased from Hello Bio (catalog #HB0225), and MPEP was obtained from Cayman Chemical (catalog #219911-35-0). AP5 was prepared in ACSF before slice recordings. MPEP was first dissolved in DMSO and diluted in ACSF before recordings. All drugs were delivered at their final concentrations via syringe pumps.

Study design and statistical analysis. All data are expressed as mean ± SEM. The sample sizes used in the study were based on our previous experience with similar studies (Finnegan et al., 2004; Zhao et al., 2012; Deng et al., 2019a) and were similar to those generally used in the field. The animals were randomly assigned (1:1 allocation) to the control and

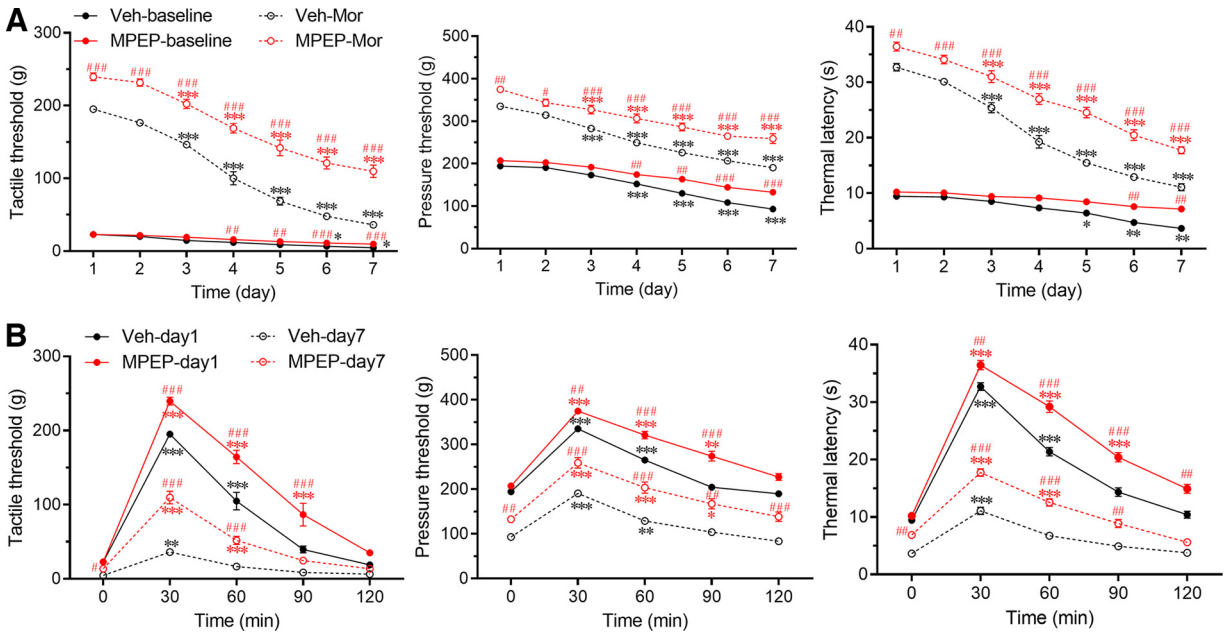

Figure 1. Blocking mGluR5 at the spinal cord level reduces morphine-induced hyperalgesia and tolerance in rats. ***A***, Time course of the effect of MPEP on hyperalgesia and tolerance induced by repeated morphine injections. Nociceptive thresholds and latency were tested before (baseline) and 30 min after (Mor) the first morphine injection every day. Rats were intraperitoneally injected with morphine (5 mg/kg) twice per day for 7 consecutive days. MPEP (60 μg) or vehicle (Veh) was intrathecally injected 10 min prior to each morphine injection daily. ***B***, Time course of the acute effect of morphine on nociception and the effect of cotreatment with MPEP. Nociceptive thresholds and latency were tested at the first morphine injection on day 1 and day 7. Data are mean ± SEM ($n = 10$ rats per group). $^{*}p < 0.05$, $^{**}p < 0.01$, $^{***}p < 0.001$ versus day 1 or minute 0. $^{\#}p < 0.05$, $^{\#\#}p < 0.01$, $^{\#\#\#}p < 0.001$ versus respective vehicle control at the same time (two-way ANOVA followed by Tukey *post hoc* test).

treatment groups as they become available. No animal died during the final experiments, and no test for outliers in the data were conducted. Data were pooled from male and female animals because no sex differences were found in the degree and time course of morphine-induced hyperalgesia and tolerance as well as presynaptic NMDAR hyperactivity in the present study and in our previous work (Deng et al., 2019a; Sun et al., 2019; S. R. Chen et al., 2022). The investigators performing the behavioral (D.J.) and electrophysiological (H.C. and S.-R.C.) experiments were blinded to the treatment groups. The evoked EPSCs and PPR were analyzed using Clampfit 10.0 software (Molecular Devices), and the amplitude of EPSCs was quantified by averaging 6 consecutive currents. Only 1 neuron was recorded from each spinal cord slice, and at least 4 mice or rats in each condition were used for recordings. Two-tailed Student's *t* tests were used to determine the differences between two groups. One-way and two-way ANOVA followed by Tukey *post hoc* tests were used to compare >2 groups. All statistical analyses were performed using Prism software (version 9; GraphPad Software). *p* values of <0.05 were considered statistically significant.

Results

mGluR5 at the spinal cord level promotes hyperalgesia and tolerance induced by prolonged treatment with morphine

To determine whether mGluR5 at the spinal cord level plays a role in both hyperalgesia and tolerance induced by prolonged morphine treatment, we administered morphine (5 mg/kg, i.p., twice per day) to adult rats for 7 consecutive days. We intrathecally injected MPEP (60 μg) or MPEP-free vehicle 10 min before each morphine injection. We examined the withdrawal thresholds or latency in response to a light touch stimulus, a noxious pressure stimulus, and a radiant heat stimulus 30 min before (baseline) and 30 min after the first morphine injection daily. Daily morphine administration in vehicle-treated rats caused a gradual reduction of the baseline withdrawal thresholds and latency, indicating the presence of mechanical and thermal hyperalgesia ($n = 10$ rats per group, Fig. 1*A*). These rats also showed a gradual decrease in the antinociceptive effect of morphine, indicating the development of analgesic tolerance (Fig. 1*A*). By comparison, cotreatment with MPEP substantially attenuated the reduction in baseline withdrawal thresholds and latency and in the analgesic effect of morphine (Fig. 1*A*).

We also determined how cotreatment with MPEP affects the acute analgesic effect of morphine on the first and seventh days of morphine administration. The thresholds and latency were tested before the first morphine injection. Morphine treatment had a transient analgesic effect, which was reflected by increases in the pressure withdrawal threshold, tactile withdrawal threshold, and thermal withdrawal latency on both days 1 and 7. The analgesic effect reached a peak at 30 min and gradually returned to the baseline level ($n = 10$ rats per group, Fig. 1*B*). Treatment with MPEP (60 μg) 10 min before each morphine injection potentiated the withdrawal thresholds and latency increased by morphine on both days 1 and 7 (Fig. 1*B*). These results suggest that mGluR5 at the spinal cord level antagonizes the opioid analgesic effect and promotes the development of opioid-induced hyperalgesia and tolerance.

Increased mGluR5 activity mediates glutamatergic input from primary afferent terminals to dorsal horn neurons augmented by morphine treatment

Increased glutamatergic input from primary sensory neurons to spinal dorsal horn neurons is critically involved in opioid-induced hyperalgesia and tolerance (H. Y. Zhou et al., 2010; Zhao et al., 2012; Deng et al., 2019b; S. R. Chen et al., 2022). We next determined whether mGluR5 plays a role in augmented glutamatergic input from primary afferent nerves to spinal dorsal horn neurons induced by repeated morphine treatment. To this end, rats were treated with morphine (5 mg/kg, i.p., twice per day) or vehicle for 7 d. The lumbar spinal cords were removed for electrophysiological recordings at the end of the treatment.

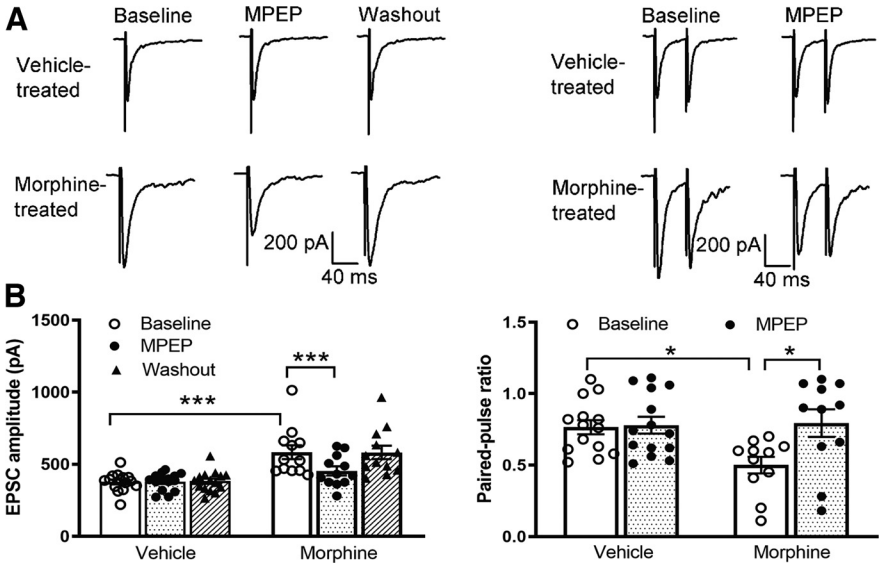

Figure 2. Inhibiting mGluR5 activity reduces glutamatergic input to the spinal cord that was increased by repeated morphine treatment in rats. ***A***, ***B***, Representative current traces (***A***) and quantitative data (***B***) show the effect of bath application of MPEP (10 μM) on the amplitude of evoked EPSCs and the PPR of evoked EPSCs in lamina II neurons from rats treated with vehicle ($n = 15$ neurons for EPSCs; $n = 14$ neurons for PPR) or morphine ($n = 12$ neurons for EPSCs; $n = 11$ neurons for PPR). Two-way ANOVA showed a significant interaction between MPEP effect and morphine treatment for the amplitude ($F_{(2,75)} = 3.866$, $p = 0.0252$) and PPR ($F_{(1,46)} = 13.78$, $p = 0.023$) of evoked EPSCs in lamina II neurons. Vehicle or morphine (5 mg/kg) was intraperitoneally injected twice per day for 7 consecutive days. Recordings were obtained from 4 rats per group. Monosynaptic EPSCs were elicited by electrical stimulation of the dorsal root. Data are mean ± SEM. *$p < 0.05$; ***$p < 0.001$; two-way ANOVA followed by Tukey *post hoc* test.

The baseline amplitude of EPSCs in spinal lamina II neurons monosynaptically evoked from the dorsal root was significantly greater in morphine-treated rats ($n = 12$ neurons) than in vehicle-treated rats ($n = 15$ neurons; 583.5 ± 48.45 vs 378.0 ± 16.78 pA, $F_{(1,75)} = 48.65$, $p < 0.001$; Fig. 2). Bath application of 10 μM MPEP for 6 min did not change the amplitude of monosynaptically evoked EPSCs in lamina II neurons from vehicle-treated rats. By contrast, application of MPEP rapidly decreased the amplitude of evoked EPSCs in lamina II neurons from morphine-treated rats (Fig. 2).

The PPR of monosynaptically evoked EPSCs of lamina II neurons was significantly lower in morphine-treated rats ($n = 11$ neurons) than in vehicle-treated rats ($n = 14$ neurons; $F_{(1,46)} = 5.463$, $p = 0.038$; Fig. 2). In lamina II neurons from morphine-treated rats, bath application of 10 μM MPEP for 6 min significantly inhibited the first evoked EPSCs more than the second evoked EPSCs, resulting in an increase in the PPR of evoked EPSCs. However, MPEP had no effect on the PPR of evoked EPSCs in lamina II neurons from vehicle-treated rats (Fig. 2). Together, these findings suggest that prolonged opioid treatment increases mGluR5 activity at primary afferent central terminals, which augments and/or maintains glutamatergic input from primary afferent nerves to spinal dorsal horn neurons.

Opposite effects of repeated treatment with opioids on mGluR5 protein levels in the DRG and spinal cord

To determine how repeated morphine exposure affects mGluR5 protein levels in the DRG and spinal cord, we collected lumbar DRGs and dorsal spinal cord tissues from mice that had been repeatedly treated with morphine (10 mg/kg, i.p., twice per day) or vehicle for 8 consecutive days (Zhao et al., 2012; Sun et al., 2019). Immunoblotting showed that in the spinal cord, mGluR5 had 2 protein bands at 130 and 260 kDa (Fig. 3*A*), which represent monomeric and dimeric mGluR5, respectively (Romano et al., 1996; D. P. Li et al., 2014). However, only the monomeric mGluR5 band at 130 kDa was detected in the DRG (Fig. 3*A*). The mGluR5 protein level in the DRG was significantly lower in morphine-treated mice than in vehicle-treated mice ($n = 6$ mice per group; $t_{(10)} = 3.945$, $p = 0.028$). By contrast, both monomeric and dimeric mGluR5 protein levels were significantly higher in the spinal cords from morphine-treated mice than from vehicle-treated mice ($n = 6$ mice per group; $t_{(10)} = 10.38$, $p < 0.0001$ in dimers; $t_{(10)} = 9.943$, $p < 0.0001$ in monomers; Fig. 3*A*,*B*). To confirm the effect of the MOR agonist on mGluR5 expression, we treated another group of mice with fentanyl (0.1 mg/kg, i.p., twice per day) for 8 consecutive days (Sun et al., 2019). Like morphine, fentanyl treatment also decreased the monomeric mGluR5 protein level in the DRG ($n = 6$ mice per group; $t_{(10)} = 3.388$, $p = 0.0069$) but increased monomeric and dimeric mGluR5 protein levels in the spinal cord ($n = 6$ mice per group; $t_{(10)} = 3.577$, $p = 0.005$ in dimers; $t_{(10)} = 4.921$, $p = 0.0005$ in monomers; Fig. 3*D*,*E*). We then used real-time PCR to examine whether prolonged treatment with MOR agonists alters the mRNA level of mGluR5 in the DRG and spinal cord in mice. Neither morphine nor fentanyl significantly changed the mGluR5 mRNA levels in the DRG or spinal cord ($n = 8$ mice per group; Fig. 3*C*,*F*).

To determine whether the effect of prolonged opioid treatment on mGluR5 protein levels in the DRG and spinal cord is species-specific, we next used rats to examine how repeated morphine administration changes mGluR5 protein levels in the DRG and spinal cord. Rats were treated with morphine (5 mg/kg, i.p., twice per day) for 7 consecutive days. As in mice, both monomeric and dimeric mGluR5 proteins were detected in the spinal cord, but only monomeric mGluR5 was present in the rat DRG (Fig. 3*G*). Morphine treatment significantly decreased mGluR5 protein levels in the DRG ($n = 6$ rats per group; $t_{(10)} = 5.125$, $p = 0.0004$) and increased monomeric and dimeric mGluR5 protein levels in the spinal cord ($n = 6$ rats per group; $t_{(10)} = 11.74$, $p < 0.0001$ in dimers; $t_{(10)} = 4.304$, $p = 0.0016$ in monomers; Fig. 3*G*,*H*). Also, treatment with morphine had no effect on the mGluR5 mRNA level in the DRG or spinal cord ($n = 6$ mice per group; Fig. 3*I*). Together, the divergent effect of prolonged opioid treatment on mGluR5 protein levels likely results from augmented mGluR5 protein trafficking from the DRG to the spinal cord.

Morphine treatment potentiates the mGluR5–NMDAR interaction and NMDAR synaptic trafficking in the spinal cord

Increased presynaptic NMDAR activity in the spinal cord is critically involved in opioid-induced hyperalgesia and tolerance (Zhao et al., 2012; Deng et al., 2019b; S. R. Chen et al., 2022). A major gap of knowledge concerns the signaling mechanisms responsible for opioid-induced NMDAR hyperactivity in the spinal cord. Functional interaction between mGluR5 and NMDARs has

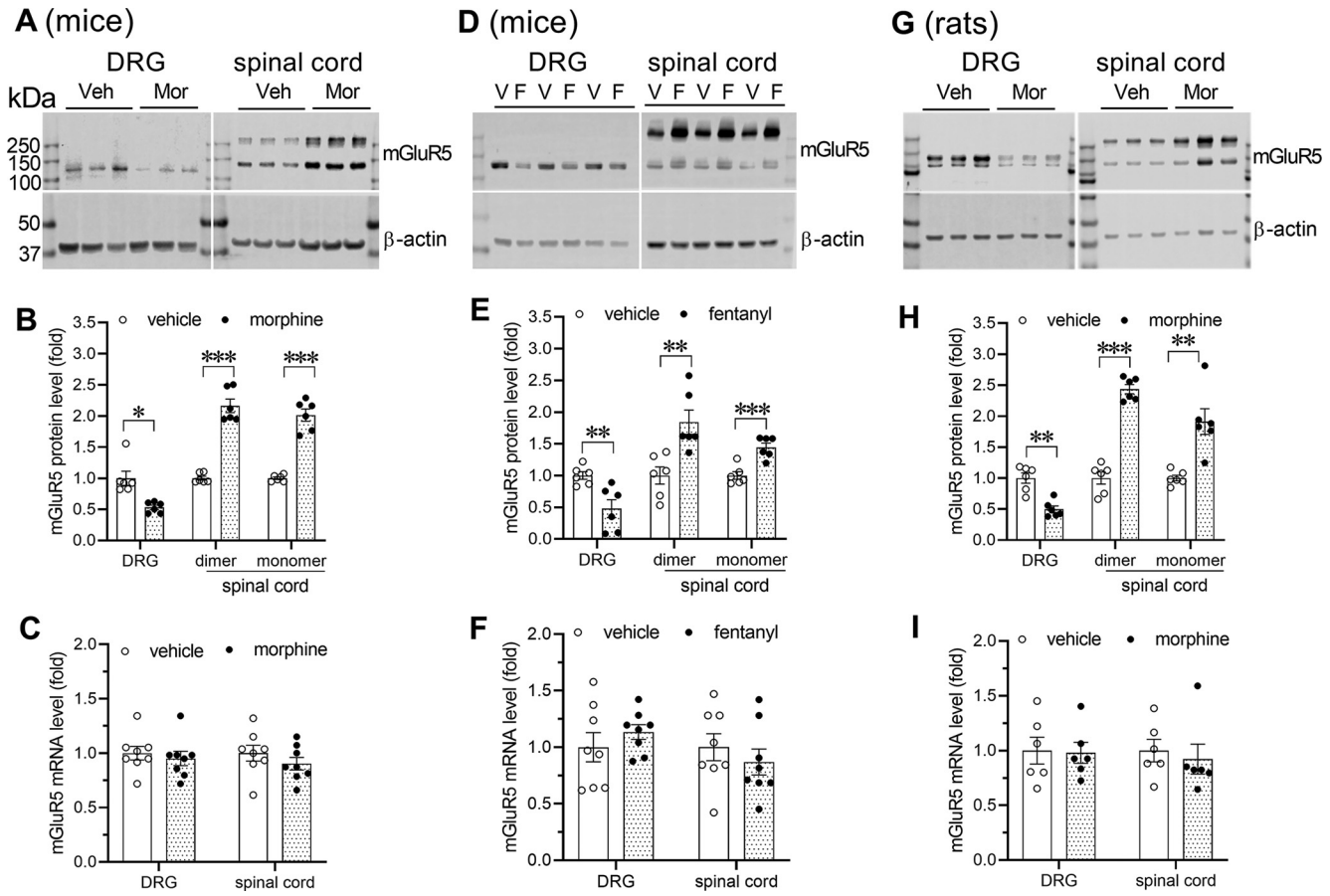

Figure 3. Repeated treatment with morphine or fentanyl produces a divergent effect on mGluR5 protein levels in the DRG and spinal cord in mice and rats. ***A***, ***B***, Representative blotting images (***A***) and quantification (***B***) show mGluR5 protein levels in the DRG and spinal cord from morphine-treated mice ($n = 6$ mice per group). ***D***, ***E***, Representative blotting images (***D***) and quantification (***E***) show mGluR5 protein levels in the DRG and spinal cord from fentanyl-treated mice ($n = 6$ mice per group). ***G***, ***H***, Representative blotting images (***G***) and quantification (***H***) show mGluR5 protein levels in the DRG and spinal cord from morphine-treated rats ($n = 6$ rats per group). ***C***, ***F***, ***I***, The mGluR5 mRNA levels in the DRG and spinal cord from morphine- (***C***) or fentanyl (***F***)-treated mice ($n = 8$ mice per group), and morphine-treated rats (***I***, $n = 6$ rats per group). Mice were intraperitoneally injected with morphine (Mor, 10 mg/kg), fentanyl (F, 0.1 mg/kg), or vehicle (Veh, V) twice per day for 8 d. Rats were intraperitoneally injected with morphine (5 mg/kg) or vehicle twice per day for 7 d. β-actin was used as a loading control. Data are mean ± SEM. *$p < 0.05$; **$p < 0.01$; ***$p < 0.001$; two-tailed Student *t* test.

been shown in the brain (Choe et al., 2006; D. P. Li et al., 2014). We therefore determined whether prolonged opioid treatment augments the physical interaction of mGluR5 with NMDARs in the spinal cord. To this end, we obtained synaptosomes from the dorsal spinal cord of rats treated with vehicle, morphine, or morphine plus MPEP. The synaptosomal proteins (input) and proteins precipitated by using an anti-mGluR5 antibody were used for immunoblotting analysis of mGluR5 and GluN1, an obligatory subunit of NMDARs (Traynelis et al., 2010). Repeated morphine treatment significantly increased monomeric and dimeric mGluR5 protein levels in the synaptosomes ($n = 6$ rats per group; $F_{(2,15)} = 5.742$, $p = 0.0193$ in dimers; $F_{(2,15)} = 2.493$, $p = 0.0082$ in monomers; Fig. 4*A*). Morphine treatment also significantly increased GluN1 protein levels in the synaptosomes of the spinal cord ($n = 6$ rats per group; $F_{(2,15)} = 5.583$, $p = 0.0195$; Fig. 4*A*). Cotreatment with MPEP did not significantly affect mGluR5 protein levels in the synaptosomes. However, cotreatment with MPEP significantly reduced the increased GluN1 protein levels in spinal synaptosomes from rats treated with morphine ($n = 6$ rats per group; $F_{(2,15)} = 5.583$, $p = 0.0466$; Fig. 4*A*). These results suggest that increased mGluR5 activity mediates opioid-augmented synaptic expression of NMDARs in the spinal cord.

Coimmunoprecipitation analysis using an anti-mGluR5 antibody showed that repeated morphine treatment significantly increased the amount of GluN1 proteins in the mGluR5 precipitates of the spinal synaptosomes ($n = 6$ rats per group; $F_{(2,15)} = 8.15$, $p = 0.0043$; Fig. 4*A*). Cotreatment with MPEP markedly reversed the amount of mGluR5-GluN1 protein complexes in the spinal synaptosomes increased by repeated morphine treatment ($n = 6$ rats per group; $F_{(2,15)} = 8.15$, $p = 0.0236$; Fig. 4*A*). These findings suggest that, via increasing mGluR5 activity, prolonged opioid treatment potentiates the mGluR5–NMDAR interaction in the spinal cord to promote synaptic NMDAR expression.

NMDARs directly interact with mGluR5 in the spinal cord but not monomeric mGluR5 in the DRG

In the above experiments, we found that mGluR5 proteins were present in monomeric and dimeric forms in the spinal cord. However, it was unclear whether monomeric or dimeric mGluR5 proteins interact with NMDARs. We used synaptosomal proteins from dorsal spinal cords to conduct reverse coimmunoprecipitation by using an anti-GluN1 antibody. Both dimeric and monomeric mGluR5 proteins were detected in the GluN1 precipitates from vehicle-treated and morphine-treated rats (Fig. 4*B*).

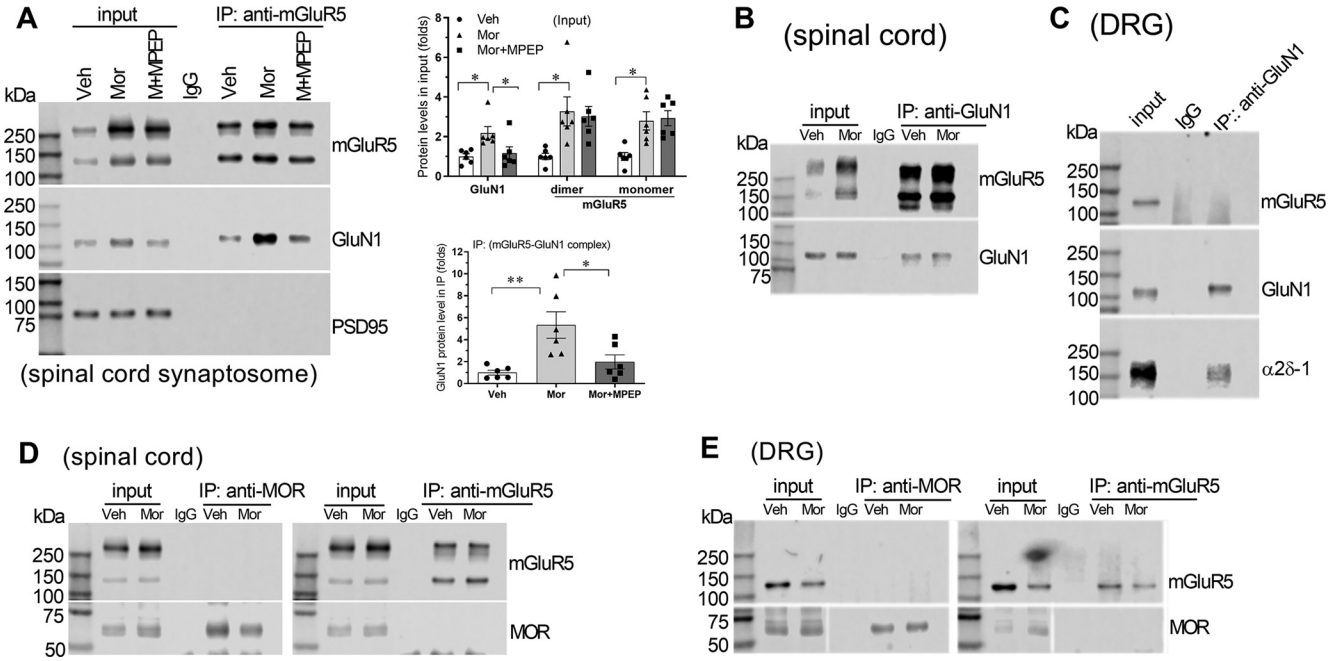

Figure 4. Inhibiting mGluR5 activity reduces the mGluR5–NMDAR interaction and NMDAR synaptic trafficking in spinal cords from rats treated with morphine. ***A***, Representative blotting images and quantification show the effects of MPEP on the protein levels of GluN1 and GluN1-mGluR5 complexes in the spinal cord synaptosome. Rats were intraperitoneally injected with morphine (Mor or M, 5 mg/kg, twice per day) or vehicle (Veh) for 7 consecutive days ($n = 6$ rats per group). MPEP (60 μg) or vehicle was intrathecally injected 10 min prior to each morphine injection daily. Synaptosomal proteins from the dorsal spinal cord were extracted for coimmunoprecipitation with an anti-mGluR5 antibody. PSD95, a synaptic protein, was used as a loading control. ***B***, Coimmunoprecipitation blotting images show that both dimeric and monomeric mGluR5 were detected in the GluN1 precipitates of spinal cords. Synaptosomal proteins from dorsal spinal cords of vehicle-treated and morphine-treated rats were extracted for immunoprecipitation with an anti-GluN1 antibody. ***C***, Coimmunoprecipitation blotting images show that GluN1 interacted with $\alpha2\delta$-1, but not mGluR5, in the DRG. Total proteins from DRG tissues were extracted for immunoprecipitation with an anti-GluN1 or anti-$\alpha2\delta$-1 antibody. ***D***, ***E***, Representative coimmunoprecipitation blotting images show that MOR proteins were not detected in the mGluR5 precipitates in the DRG (***D***) or spinal cord (***E***). Total proteins from rat DRG and dorsal spinal cord tissues were extracted for immunoprecipitation with an anti-mGluR5 antibody and immunoblotting with an anti-MOR antibody. Reverse coimmunoprecipitation was also conducted with an anti-MOR antibody for immunoprecipitation and an anti-mGluR5 antibody for immunoblotting. Rats were intraperitoneally injected with morphine (5 mg/kg, twice per day) or vehicle for 7 consecutive days. Data are mean ± SEM. $^*p < 0.05$; $^{**}p < 0.01$; one-way ANOVA followed by Tukey *post hoc* test.

Because only monomeric mGluR5 existed in the DRG (Fig. 3), we determined whether the monomeric mGluR5 physically interacts with NMDARs. We collected lumbar DRGs from rats and extracted total proteins for coimmunoprecipitation by using an anti-GluN1 antibody. However, immunoblotting did not detect any mGluR5 protein bands in the GluN1 precipitates from the rat DRG tissues (Fig. 4*C*). $\alpha2\delta$-1 directly interacts with NMDARs via its C terminus, an intrinsically disordered protein region (J. Chen et al., 2018; Y. Chen et al., 2019). The $\alpha2\delta$-1–NMDAR interaction in the spinal cord and brain has been demonstrated previously (Y. Huang et al., 2020; J. J. Zhou et al., 2021a). As a positive control, we detected an $\alpha2\delta$-1 protein band in the GluN1 precipitates from the DRG (Fig. 4*C*). These results indicate that NMDARs physically interact with mGluR5 in the spinal cord but not monomeric mGluR5 in the DRG.

Endogenous mGluR5 and MOR proteins do not physically interact in the DRG or spinal cord

The above experiments showed that increased mGluR5 activity plays a key role in opioid-induced hyperalgesia and augmented glutamatergic input from primary afferent nerves to the spinal dorsal horn (Figs. 1 and 2). We next attempted to define how MOR stimulation increases mGluR5 activity or trafficking. mGluR5 and MOR proteins seem to interact when they are overexpressed in HEK293 cells (Schroder et al., 2009). We determined whether mGluR5 interacts with MORs *in vivo* by using coimmunoprecipitation. In the mGluR5 precipitates, no MOR-immunoreactive band was detected in either the DRG or spinal cord tissues from vehicle- and morphine-treated mice (Fig. 4*D*,*E*). Furthermore, in the reverse coimmunoprecipitation assay using a specific MOR antibody, no mGluR5 immunoreactivity was present in the MOR precipitates in either the DRG or spinal cord tissues (Fig. 4*D*,*E*). Thus, these data indicate that mGluR5 and MOR proteins do not directly interact in the DRG or spinal cord.

Validation of lentiviral vectors expressing mGluR5-specific gRNA *in vitro* and *in vivo*

Because intrathecally administered agents readily access both the DRG and spinal cord neurons (Cai et al., 2009), it is not possible to differentiate the role of mGluR5 in the DRG and spinal cord in opioid-induced hyperalgesia and tolerance in this way. To specifically determine the role of mGluR5 expressed in primary sensory neurons in the development of opioid-induced hyperalgesia and tolerance, we produced mice with conditional mGluR5 knockdown in DRG neurons using a Clustered Regularly Interspaced Short Palindromic Repeats (CRISPR)-Cas9 approach. To this end, we cloned 4 mGluR5 gRNAs, each of which targeted a different location in the mouse mGluR5 gene (*Grm5*), into lentiGuide-Puro plasmids. These gRNA-containing plasmids were then cotransfected with a pcDNA6 plasmid containing the complete mouse *Grm5* coding sequence and lentiCas9-EGFP plasmids in HEK293FT cells. After 3 d of coincubation, the cells were collected for immunoblotting analysis with an anti-mGluR5 antibody. All four gRNAs markedly reduced monomeric and

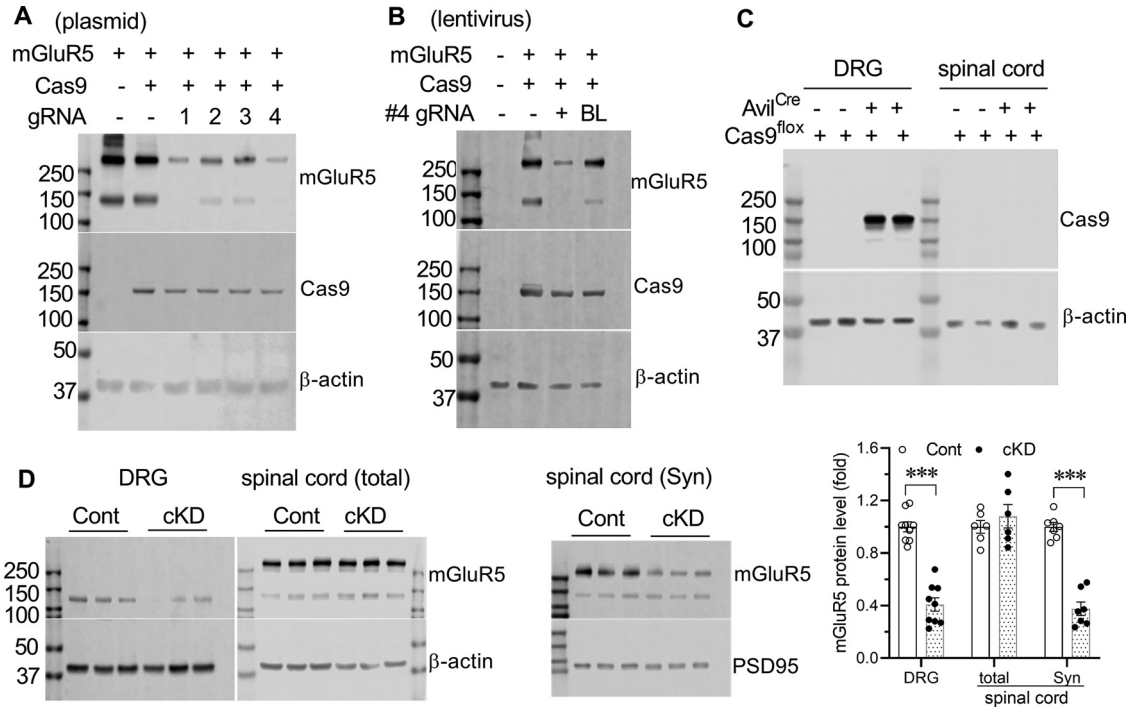

Figure 5. Validation of the mGluR5 gRNA and CRISPR-Cas9–induced mGluR5 ablation *in vitro* and *in vivo*. ***A***, Representative blotting images show the effect of four different mGluR5 gRNAs on mGluR5 protein levels in a cell line. HEK293FT cells were cotransfected with an mGluR5-pcDNA6 plasmid (mGluR5), a lenti-Cas9 plasmid (Cas9), and lentiGuide-Puro plasmids containing four different mGluR5 gRNAs. After 3 d of coincubation with the plasmids, the cells were collected, and proteins were extracted for immunoblotting analysis. ***B***, Representative blotting images show the effect of the mGluR5 gRNA-expressing lentivirus on mGluR5 protein levels in a cell line. HEK293FT cells were cotransfected with an mGluR5-pcDNA6 plasmid and lenti-Cas9 plasmid. On the second day, the cells were washed, and the medium was refreshed. The packaged lentivirus containing mGluR5 gRNA or nonpackaged gRNA alone (BL) was added to the cell culture medium. Three days later, the cells were collected, and proteins were extracted for immunoblotting analysis. ***C***, Representative blotting images show the Cas9 proteins were detected in the DRG, but not the spinal cord, in *Avil*$^{Cre/+}$::Cas9$^{Flox/+}$ mice. Total proteins were extracted for immunoblotting analysis to confirm Cas9 expression. ***D***, Representative blotting images and quantification show the differential effect of the mGluR5 gRNA-expressing lentivirus on mGluR5 protein levels in the DRG and dorsal spinal cords from *Avil*$^{Cre/+}$::Cas9$^{Flox/+}$ mice. The mGluR5 gRNA-expressing lentivirus or control lentivirus (Cont) was injected intrathecally in conditional Cas9 knock-in (*Avil*$^{Cre/+}$::Cas9$^{Flox/+}$) mice. After 20 d, the DRG and dorsal spinal cords were obtained, and total proteins and synaptosomal (Syn) proteins were extracted for immunoblotting analysis of mGluR5 expression ($n = 6$ mice per group). Data are mean ± SEM. ***$p < 0.001$ (two-tailed Student *t* test).

dimeric mGluR5 protein levels in the presence of Cas9 (Fig. 5*A*). Because the #4 mGluR5 gRNA was the most effective one, it was selected and used for the following experiments.

We packaged the lentiGuide-Puro plasmid containing #4 gRNA (sequence and location in mouse *Grm5*: 4453-*CGG CCATCGAGGTGACCGG*-4471) into a lentivirus through cotransfection with packaging plasmids in HEK293FT cells. Three days later, the medium containing the virus was collected. The medium from HEK293FT cells that had been transfected with the mGluR5 gRNA plasmid, but without packaging plasmids, was also collected as a no-virus control. To determine the efficacy of the mGluR5 gRNA-containing lentivirus, we cotransfected mGluR5-pcDNA6 and lentiCas9 plasmids into new HEK293FT cells to express mGluR5 and Cas9. On the second day, the cells were washed, and the medium was replaced with fresh medium. The mGluR5 gRNA lentivirus-containing medium or no-virus control medium were directly added to these cells. After 3 d of coculture, the cells were collected to examine mGluR5 protein levels. Only coculture with well-packaged gRNA-containing lentivirus reduced mGluR5 expression (Fig. 5*B*). These results confirmed the successful construction of an active mGluR5 gRNA-containing lentivirus.

We next determined the effect of this mGluR5 gRNA-expressing lentivirus on mGluR5 expression in the DRG and spinal cord. Cas9 proteins were detected in the DRG, but not spinal cord, obtained from *Avil*$^{Cre/+}$::Cas9$^{Flox/+}$ mice (Fig. 5*C*). Thus, the *Avil*$^{Cre/+}$::Cas9$^{Flox/+}$ mice were considered to have conditional Cas9 knock-in in DRG neurons. We then intrathecally injected mGluR5 gRNA-expressing lentivirus or negative control virus into *Avil*$^{Cre/+}$::Cas9$^{Flox/+}$ mice at the lumbar spinal level. Twenty days later, the DRG (L4-L6) and dorsal lumbar spinal cords were obtained from the mice, and the total proteins and synaptosomal proteins were extracted for immunoblotting analysis. The mGluR5 gRNA-expressing lentivirus diminished mGluR5 protein levels in the DRG compared with the control virus ($n = 9$ mice per group; $t_{(16)} = 9.277$, $p < 0.0001$; Fig. 5*D*). In the spinal cord, monomeric or dimeric mGluR5 protein levels did not differ significantly between mice injected with the mGluR5 gRNA-expressing virus and those injected with the control virus. However, injection of the mGluR5 gRNA-expressing virus markedly decreased dimeric mGluR5 protein levels in spinal cord synaptosomes ($n = 6$ mice per group; $t_{(12)} = 10.16$, $p < 0.001$; Fig. 5*D*). These data indicate that intrathecal delivery of mGluR5 gRNA using the lentivirus in *Avil*$^{Cre/+}$::Cas9$^{Flox/+}$ mice effectively diminishes mGluR5 expression in the DRG and synaptic expression of mGluR5 dimers at primary afferent terminals in the spinal cord.

Conditional mGluR5 knockdown in DRG neurons diminishes synaptic expression of mGluR5 and NMDARs in the spinal cord increased by morphine treatment

Given our finding that treatment with morphine increased mGluR5 trafficking from the DRG to spinal cord, we used

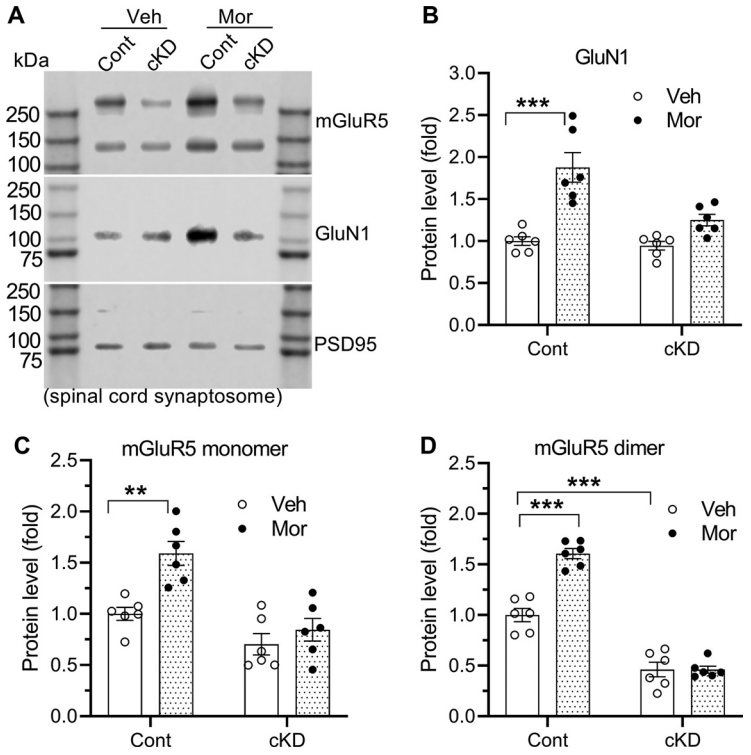

Figure 6. Conditional mGluR5 knockdown in DRG neurons diminishes morphine treatment-potentiated synaptic expression of mGluR5 and NMDARs in the spinal cord. ***A–D***, Representative blotting images (***A***) and quantification (***B-D***) show the effect of morphine treatment on protein levels of mGluR5 and GluN1 in spinal cord synaptosomes from mGluR5-cKD mice and control lentivirus (Cont) injected mice. Two-way ANOVA showed a significant interaction between mGluR5-cKD and morphine treatment ($F_{(1,20)} = 8.058$, $p = 0.0101$ in ***B***; $F_{(1,20)} = 4.985$, $p = 0.0372$ in ***C***; and $F_{(1,20)} = 27.91$, $p < 0.0001$ in ***D***). mGluR5-cKD mice were generated by intrathecal injection of lentiviral vectors expressing mGluR5-specific gRNA in conditional Cas9 knock-in ($Avil^{Cre/+}$::$Cas9^{Flox/+}$) mice. After 20 d, mGluR5-cKD mice and control lentivirus (Cont) injected $Avil^{Cre/+}$::$Cas9^{Flox/+}$ mice were intraperitoneally injected with morphine (Mor, 10 mg/kg, twice per day) or vehicle (Veh) for 8 consecutive days. Dorsal lumbar spinal cord tissues were collected, and synaptosomal proteins were used for immunoblotting analysis of mGluR5 and GluN1. PSD95, a synaptic protein, was used as a loading control. Data are mean ± SEM ($n = 6$ mice per group). **$p < 0.01$; ***$p < 0.001$; two-way ANOVA followed by Tukey *post hoc* test.

CRISPR-Cas9–induced conditional mGluR5 knockdown (mGluR5-cKD) mice to determine whether mGluR5 produced in DRG neurons plays a role in synaptic trafficking of mGluR5 and NMDARs in the spinal cord potentiated by morphine treatment. We intrathecally injected $Avil^{Cre/+}$::$Cas9^{Flox/+}$ mice with the mGluR5 gRNA-expressing lentivirus or negative control lentivirus at the lumbar level. Twenty days later, the mGluR5-cKD mice and mice injected with control virus were treated with morphine (10 mg/kg, i.p., twice per day) for 8 d. The mice were then killed, and dorsal lumbar spinal cords were collected. Immunoblotting analysis of spinal synaptosomes showed that morphine treatment significantly increased GluN1 protein levels in control virus-treated mice ($n = 6$ mice per group, $F_{(1,20)} = 34.53$, $p < 0.0001$; Fig. 6*A*,*B*). mGluR5-cKD did not alter GluN1 levels in the spinal synaptosomes obtained from vehicle-treated mice. However, mGluR5-cKD blocked the potentiating effect of morphine treatment on GluN1 protein levels in the spinal synaptosomes ($n = 6$ mice per group). Furthermore, mGluR5-cKD significantly decreased dimeric mGluR5 protein levels in the spinal synaptosomes from vehicle-treated mice ($n = 6$ mice per group, $F_{(1,20)} = 213.7$, $p < 0.0001$). Remarkably, repeated treatment with morphine significantly increased monomeric and dimeric mGluR5 protein levels in the spinal synaptosomes from control virus-treated mice ($F_{(1,20)} = 27.66$, $p < 0.0001$ in dimers; $F_{(1,20)} = 13.18$, $p = 0.0026$ in monomers) but not from mGluR5-cKD mice ($n = 6$ mice per group; Fig. 6*A*,*C*,*D*). These findings suggest that mGluR5 expressed in DRG neurons mediates augmented synaptic trafficking of NMDARs and mGluR5 in the spinal cord induced by opioid treatment.

mGluR5 in DRG neurons is compulsory for morphine treatment-induced presynaptic NMDAR hyperactivity in the spinal dorsal horn

We then determined whether mGluR5 produced in DRG neurons plays a role in opioid-induced potentiation of NMDAR-mediated primary afferent input to spinal dorsal horn neurons. We first generated mGluR5-cKD and control mice via intrathecal injection of lentiviral vectors expressing mGluR5-specific gRNA and control lentiviral vectors, respectively, in $Avil^{Cre/+}$::$Cas9^{Flox/+}$ mice. Twenty days later, these mice were treated with morphine (10 mg/kg, i.p., twice per day) for 7 d. The lumbar spinal cords were then removed for whole-cell patch-clamp recordings. Treatment with morphine significantly increased the baseline amplitude of EPSCs of lamina II neurons monosynaptically evoked from the dorsal root in control lentivirus-treated mice ($n = 15$ neurons) compared with mice that received morphine-free vehicle plus control lentivirus ($n = 16$ neurons; $F_{(1,87)} = 17.891$, $p = 0.0022$; Fig. 7). CRISPR-Cas9–induced mGluR5-cKD ($n = 15$ neurons) normalized the morphine treatment-elevated baseline amplitude of monosynaptically evoked EPSCs of lamina II neurons to the level of the vehicle-treated group. NMDAR-mediated EPSCs of lamina II neurons were assessed using AP5, a specific NMDAR antagonist. Bath application of 50 μM AP5 for 6 min markedly reduced the morphine-elevated amplitude of monosynaptically evoked EPSCs of lamina II neurons from control lentivirus-injected mice. However, AP5 had no such effect on evoked EPSCs of lamina II neurons from mGluR5-cKD mice treated with morphine (Fig. 7).

To determine the presynaptic action of mGluR5-cKD, we also examined the PPR of monosynaptically evoked EPSCs in spinal dorsal horn neurons from morphine-treated mice. Compared with vehicle-treated mice ($n = 16$ neurons), treatment with morphine in control lentivirus-injected mice ($n = 15$ neurons) significantly increased the first evoked EPSCs more than the second evoked EPSCs, resulting in a decrease in the PPR of evoked EPSCs in lamina II neurons ($F_{(1,58)} = 7.242$, $p = 0.0248$; Fig. 7). This morphine-induced decrease in the PPR of evoked EPSCs was not observed in neurons from mGluR5-cKD mice (Fig. 7). Furthermore, bath application of 50 μM AP5 rapidly reversed this morphine treatment-induced PPR decrease in lamina II neurons in control lentivirus-injected mice. By contrast, AP5 had no such effect in mGluR5-cKD mice treated with morphine (Fig. 7). Together, these findings suggest that mGluR5 expressed in DRG neurons is required for presynaptic NMDAR hyperactivity and the associated increase in glutamatergic input

from primary afferents to spinal dorsal horn neurons induced by opioid treatment.

Conditional knockdown of mGluR5 in DRG neurons attenuates morphine-induced hyperalgesia and tolerance

Last, we determined whether mGluR5 expressed in DRG neurons plays a role in morphine-induced hyperalgesia and tolerance. $Avil^{Cre/+}$::$Cas9^{Flox/+}$ mice were intrathecally injected with lentiviral vectors expressing mGluR5-specific gRNA (mGluR5-cKD) or control lentiviral vectors. Twenty days after lentivirus injection, these mice were treated with morphine (10 mg/kg, i.p., twice per day) for 8 consecutive days. The pressure and tactile withdrawal thresholds and thermal withdrawal latency were examined before (baseline) and 30 min after the first morphine injection daily. The time course of the acute analgesic effect of the first morphine injection was also tested on the first and eighth days. Before starting morphine treatment, the baseline pressure and tactile withdrawal thresholds and thermal withdrawal latency did not differ significantly between mGluR5-cKD mice ($n = 9$ mice) and control lentivirus-injected mice ($n = 7$ mice, Fig. 8*A*).

As in rats (Fig. 1), daily morphine treatment in control lentivirus-injected mice caused a gradual reduction in the baseline mechanical withdrawal thresholds and thermal withdrawal latency measured before daily morphine injection, indicating the presence of hyperalgesia. Daily morphine treatment in control lentivirus-injected mice also caused a gradual decrease in the acute analgesic effect of morphine ($n = 7$ mice, Fig. 8*A*), indicating the development of analgesic tolerance. In mGluR5-cKD mice ($n = 9$ mice), although there was a gradual reduction over time in the pressure and tactile withdrawal thresholds and thermal latency at the baseline level, the baseline withdrawal thresholds and latency were significantly higher than in control lentivirus-injected mice on the same days (Fig. 8*A*). Furthermore, the reduction in the acute analgesic effect of morphine was significantly less in mGluR5-cKD mice than in control lentivirus-injected mice (Fig. 8*A*).

Morphine treatment in control lentivirus-injected mice produced a transient increase in pressure and tactile withdrawal thresholds and thermal latency when tested on the first and eighth day. These acute analgesic effects of morphine were greater in mGluR5-cKD mice ($n = 9$ mice) than in control lentivirus-injected mice ($n = 7$ mice, Fig. 8*B*). These results suggest that mGluR5 from DRG neurons counteracts the opioid analgesic effect and promotes the development of opioid-induced hyperalgesia and tolerance.

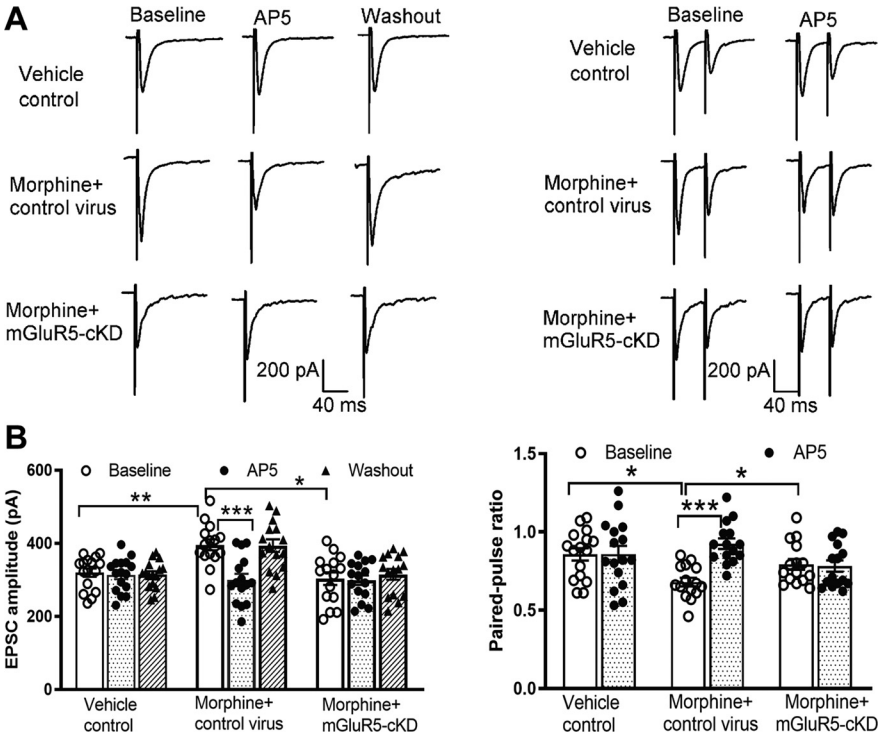

Figure 7. Conditional mGluR5 knockdown in DRG neurons eliminates NMDAR-mediated glutamatergic input from primary afferents to the spinal cord that was increased by morphine treatment. ***A***, ***B***, Representative current traces (***A***) and quantification (***B***) show EPSCs evoked monosynaptically from dorsal root stimulation and PPR of evoked EPSCs in lamina II neurons from mice injected with mGluR5 gRNA-expressing lentivirus (mGluR5-cKD) or control virus and then subjected to treatment with vehicle ($n = 16$ neurons) or morphine ($n = 15$ neurons in both mGluR5-gRNA lentivirus and control lentivirus groups). Two-way ANOVA showed a significant interaction between mGluR5-cKD and AP5 treatment for the amplitude ($F_{(2,28)} = 18.77$, $p < 0.001$) and PPR ($F_{(1,14)} = 13.78$, $p = 0.0023$) of evoked EPSCs. Conditional Cas9 knock-in ($Avil^{Cre/+}$::$Cas9^{Flox/+}$) mice were intrathecally injected with mGluR5 gRNA-expressing lentivirus (mGluR5-cKD) or control virus. After 20 d, these mice were intraperitoneally injected with morphine (10 mg/kg, twice per day) for 7 d. Recordings were obtained from 4 mice per group. Monosynaptic EPSCs were elicited by electrical stimulation of the dorsal root. Data are mean ± SEM. *$p < 0.05$; **$p < 0.01$; ***$p < 0.001$; two-way ANOVA followed by Tukey *post hoc* test.

Discussion

Our study reveals that mGluR5 from primary sensory neurons mediates opioid-induced hyperalgesia and tolerance. In the present study, we found that intrathecally injected MPEP attenuated both hyperalgesia and tolerance caused by prolonged morphine treatment, suggesting an important role of mGluR5 at the spinal level in these opioid adverse effects. To specifically determine the contribution of mGluR5 originating from DRG neurons, we used a CRISPR-Cas9–mediated gene editing strategy to induce conditional mGluR5 knockdown in DRG neurons. We first generated $Avil^{Cre/+}$::$Cas9^{Flox/Flox}$ mice in which Cas9 was expressed in DRG neurons. We then intrathecally injected lentiviral vectors expressing a validated mGluR5-specific gRNA to induce conditional mGluR5 knockdown in DRG neurons. Because Cas9 is not expressed in the spinal cord of $Avil^{Cre/+}$::$Cas9^{Flox/Flox}$ mice, the gRNA injected intrathecally selectively ablated mGluR5 in DRG neurons. The advantage of this approach is that it circumvents unintended ectopic gene KO caused by Cre expression in other cells/tissues of $Avil^{Cre/+}$ mice, such as the sympathetic ganglion (Hunter et al., 2018). Intrathecal administration of lentiviral vectors transfects ~94% DRG neurons (L. Li et al., 2016). Also, $Avil^{Cre/+}$-induced gene KO occurs in ~84% of DRG neurons (Zappia et al., 2017), which accounts for the incomplete removal of mGluR5 in the DRG produced by the CRISPR-Cas9 approach. Like MPEP, conditional mGluR5 knockdown in DRG neurons reduced morphine-induced hyperalgesia and tolerance. Further evidence of the involvement of mGluR5 from primary sensory neurons

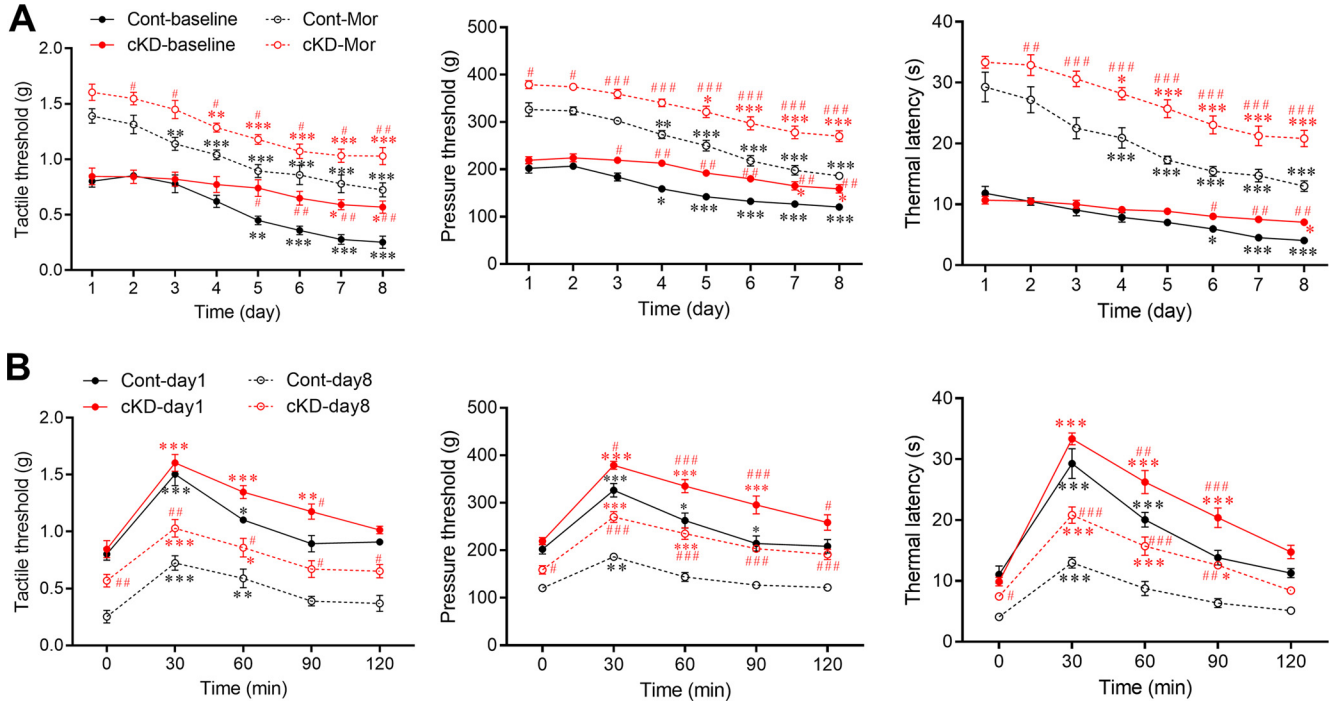

Figure 8. Conditional mGluR5 knockdown in DRG neurons attenuates hyperalgesia and tolerance induced by repeated morphine treatment. ***A***, Time course of the effect of conditional knockdown of mGluR5 (mGluR5-cKD) in DRG neurons on morphine-induced hyperalgesia and tolerance. Nociceptive thresholds and latency were tested before (baseline) and 30 min after the first morphine injection (Mor) daily. ***B***, Time course of the acute analgesic effect produced by the first morphine injection on day 1 and day 8 in CRISPR/Cas9-mediated mGluR5-cKD mice and control mice treated with repeated morphine injections. mGluR5-cKD mice were generated by intrathecal injection of lentiviral vectors expressing mGluR5-specific gRNA in conditional Cas9 knock-in ($Avil^{Cre/+}$::$Cas9^{Flox/+}$) mice. Twenty days later, mGluR5-cKD mice ($n = 9$ mice) and $Avil^{Cre/+}$::$Cas9^{Flox/+}$ mice injected with a control virus ($n = 7$ mice) were intraperitoneally injected with morphine (10 mg/kg, twice per day) for 8 consecutive days. Data are mean ± SEM. $^{*}p < 0.05$, $^{**}p < 0.01$, $^{***}p < 0.001$ versus day 1 or minute 0. $^{\#}p < 0.05$, $^{\#\#}p < 0.01$, $^{\#\#\#}p < 0.001$ versus respective control groups at the same time (two-way ANOVA followed by Tukey *post hoc* test).

in opioid-induced hyperalgesia and tolerance was provided by studies using chemical ablation of TRPV1-expressing neurons. Ablating TRPV1-expressing neurons not only potentiates the opioid analgesic effect but also diminishes opioid-induced LTP in the spinal cord, hyperalgesia, and tolerance (S. R. Chen and Pan, 2006; S. R. Chen et al., 2007; H. Y. Zhou et al., 2010). Because mGluR5 is coexpressed with TRPV1 in DRG neurons (Kim et al., 2009), ablating TRPV1-expressing neurons likely eliminates mGluR5 in DRG neurons and their afferent terminals, thereby attenuating opioid-induced hyperalgesia and tolerance.

A salient finding of our study is that prolonged opioid exposure promotes anterograde trafficking of mGluR5 from DRG neurons to their afferent terminals in the spinal cord. Trafficking of Group I mGluRs (mGluR1 and mGluR5) plays crucial roles in controlling the precise spatiotemporal localization and activity of these receptors, both of which are important for proper downstream signaling (Ojha et al., 2022; Scheefhals et al., 2023). mGluR5 is trafficked to synapses and plasma membranes of neurons in response to various stimuli (D. P. Li et al., 2014; Bodzęta et al., 2021). mGluR5 is expressed in DRG neurons and the spinal dorsal horn (Hudson et al., 2002). In the superficial dorsal horn, mGluR5 is present predominantly at primary afferent terminals (Valerio et al., 1997; Aronica et al., 2001). In the present study, we found that conditional mGluR5 knockdown in DRG neurons markedly reduced dimeric mGluR5 levels in spinal synaptosomes, suggesting that DRG neurons likely synthesize mGluR5 and provide a major reservoir of mGluR5 proteins for the anterograde transport to primary afferent central terminals. Similarly, conditional KO of *Oprm1*, *Oprd1*, or *Grin1* in DRG neurons also reduces the expression of the respective proteins in the spinal dorsal horn (Sun et al., 2019; Y. Huang et al., 2020; Jin et al., 2022). We found unexpectedly that repeated treatment with morphine or fentanyl reduced mGluR5 protein levels in the DRG but increased its abundance in the dorsal spinal cord, without affecting the mGluR5 mRNA level in either tissue. Importantly, we demonstrated that morphine treatment failed to increase mGluR5 levels in spinal synaptosomes in mice with mGluR5 knockdown in DRG neurons. This finding provides further evidence for potentiated anterograde trafficking of mGluR5 from DRG neurons to their central terminals in response to opioid treatment.

It remains enigmatic as to how opioid treatment potentiates mGluR5 trafficking from DRG neurons to their central terminals in the spinal cord. Although an association of MORs with mGluR5 was reported in HEK293 cells (Schroder et al., 2009), we did not detect a direct interaction between these two receptors in the DRG or spinal cord, suggesting that MORs do not physically interact with mGluR5 *in vivo*. Increased mGluR5 phosphorylation by PKC potentiates surface trafficking of mGluR5 in cultured hippocampal neurons and cell lines (Ko et al., 2012). Because treatment with opioids increases PLC and PKC activity in DRG neurons (Xie et al., 1999), this may lead to mGluR5 phosphorylation to augment mGluR5 trafficking from DRG neurons to spinal cord synapses. In addition, motor proteins, such as dyneins and kinesins, are actively involved in the surface/membrane transport of proteins in the DRG and spinal cord (S. R. Chen et al., 2014b; Higerd-Rusli et al., 2023). Further studies are needed to define whether opioids affect the interplay between mGluR5 and motor proteins.

Interestingly, we showed in this study that only monomeric mGluR5 was detected in the DRG, whereas both monomeric and

dimeric forms of mGluR5 existed in the dorsal spinal cord. Many mGluRs can form homodimers or heterodimers in various cells and tissues (Romano et al., 1996; J. Lee et al., 2020). Oligomerization allows proteins to form large structures without increasing the genome size and provides stability (Palczewski, 2010). Decreasing dimeric formation of mGluR1 reduces the ability of the receptor coupling to facilitate phosphoinositide turnover (Hermans and Challiss, 2001). Also, mGluR2, a Group II mGluR, activates G proteins on glutamate binding only as a full-length dimer (El Moustaine et al., 2012). Monomers and dimers of mGluR5 proteins are expressed in the brain (Romano et al., 1996; D. P. Li et al., 2014). mGluR5 is a glycosylated protein (Bhave et al., 2003) and exists as dimers at the cell surface through disulfide bonds and glycosylation (Romano et al., 1996; Copani et al., 2000; Hermans and Challiss, 2001). The important function of dimeric mGluR5 is supported by the finding that disrupting mGluR5 dimers with reducing agents attenuates their response to an mGluR5 agonist in hippocampal slices, cerebellar granule cells, and mGluR5-expressing fibroblasts (Copani et al., 2000). It is likely that, in the spinal dorsal horn, functional mGluR5 are largely expressed as homodimers on synaptic membranes, whereas monomeric mGluR5 proteins mainly reside in the endoplasmic reticulum or other intracellular compartments.

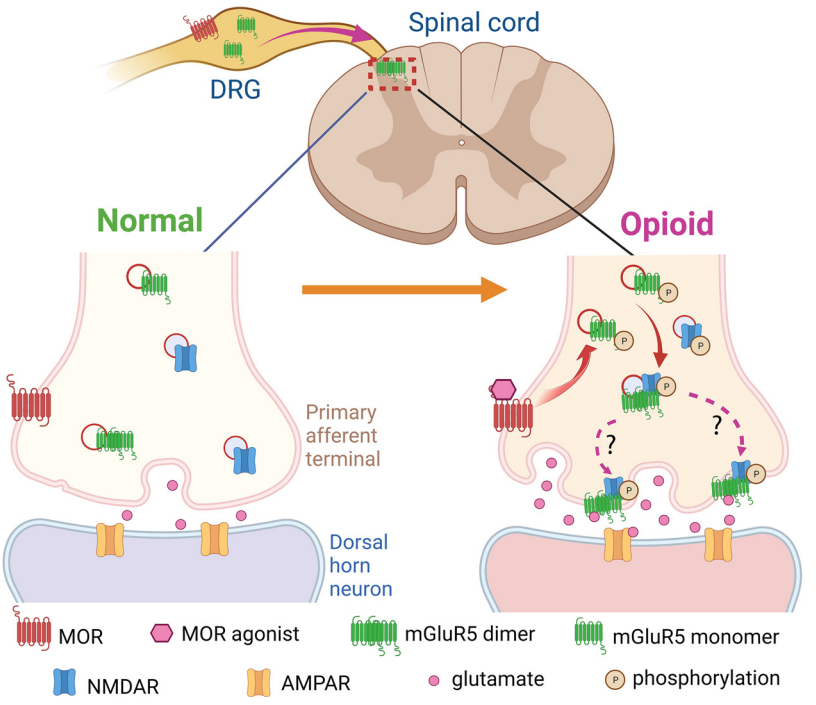

Figure 9. Schematic representation shows the potential role of mGluR5 from primary sensory neurons in opioid-induced potentiation in presynaptic expression and activity of NMDARs in the spinal dorsal horn. Under normal conditions, mGluR5 and NMDARs are minimally phosphorylated and show little interaction inside primary afferent central terminals. Prolonged opioid treatment promotes phosphorylation and trafficking of mGluR5 proteins from DRG neurons to their central terminals in the spinal dorsal horn. In the spinal cord, the trafficked mGluR5 proteins dimerize and form a protein complex with phosphorylated NMDARs and subsequently potentiate synaptic expression and activity of NMDARs at primary afferent terminals. Also, the opioid-induced increase in synaptic glutamate release may act on presynaptic mGluR5 to promote and stabilize phosphorylation of mGluR5 and NMDARs to sustain their synaptic expression. Consequently, mGluR5 and NMDARs mutually augment glutamatergic input to spinal dorsal horn neurons, leading to hyperalgesia and the loss of opioid analgesic efficacy. Further validation is needed for opioid-induced phosphorylation and synaptic trafficking steps of mGluR5 and NMDARs at primary afferent terminals. MOR, μ-opioid receptor; AMPAR, AMPA receptor.

Another important finding of our study is that mGluR5 formed a heteromeric protein complex with NMDARs in the spinal cord, which was augmented by opioid treatment. By contrast, monomeric mGluR5 present in the DRG did not interact with NMDARs. It can thus be inferred that NMDARs interact predominantly with dimeric mGluR5 in the spinal cord. Functional interactions between mGluR5 and NMDARs in the brain are suggested by previous reports (Mao and Wang, 2002; Yang et al., 2004; D. P. Li et al., 2014). We showed in this study that morphine treatment increased the amount of synaptic mGluR5–NMDAR complexes, whereas inhibition of mGluR5 with MPEP reversed this increase, suggesting that increased mGluR5 activity is important for the mGluR5–NMDAR interaction augmented by morphine treatment. It is possible that only dimeric mGluR5 proteins in the spinal cord are functionally active in the synaptic expression and interaction with NMDARs promoted by opioids. Although both dimeric and monomeric mGluR5 were observed in GluN1 precipitates in the spinal cord, the use of DTT and SDS in the coimmunoprecipitation assay likely denatured and disrupted mGluR5 dimers. Interestingly, $\alpha 2\delta$-1, another protein critically involved in opioid-induced NMDAR hyperactivity (Deng et al., 2019a; S. R. Chen et al., 2022), mainly interacts with phosphorylated GluN1/2A and GluN1/2B heterodimers, but not individual NMDAR subunits (J. Chen et al., 2018; M. H. Zhou et al., 2021b). Through protein oligomerization, mGluR5, $\alpha 2\delta$-1, and phosphorylated NMDARs may function as a large, multimeric signaling complex at the spinal cord level to initiate and sustain opioid-induced hyperalgesia and tolerance.

We further uncovered that mGluR5, via dynamic interaction with NMDARs, is required for opioid-induced presynaptic NMDAR hyperactivity in the spinal cord. Increased mGluR5 activity potentiates glutamatergic input to spinal dorsal horn neurons in neuropathic pain (J. Q. Li et al., 2010; Xie et al., 2017). Augmented NMDAR activity at primary afferent central terminals is crucial to opioid-induced hyperalgesia and tolerance by potentiating nociceptive input to spinal dorsal horn neurons (Zhao et al., 2012; Deng et al., 2019a; S. R. Chen et al., 2022). Consistent with these findings, we showed in this study that morphine treatment increased presynaptic NMDAR activity, reflected by the increased amplitude of NMDAR-mediated monosynaptic EPSCs evoked from the dorsal root and the decreased PPR of EPSCs in dorsal horn neurons. Furthermore, morphine treatment increased synaptic expression of NMDARs in the spinal cord. These morphine-induced changes were reversed by either MPEP or conditional mGluR5 knockdown in DRG neurons. Therefore, increased activity of mGluR5, originating from DRG neurons, is integral to opioid-induced presynaptic NMDAR hyperactivity in the spinal dorsal horn via promoting/sustaining NMDAR synaptic expression. We showed in this study that inhibiting mGluR5 activity with MPEP not only diminished the mGluR5 interaction with NMDARs but also reversed NMDAR synaptic trafficking potentiated by opioid exposure. Because bath application of MPEP reversed the increased amplitude of EPSCs of dorsal horn neurons by morphine

treatment, continued mGluR5 signaling is probably required for maintaining or stabilizing synaptic expression of mGluR5–NMDAR complexes in the spinal dorsal horn and presynaptic NMDAR activity augmented by opioids. This mGluR5 activity may sustain PKC-meditated NMDAR phosphorylation, which is pivotal for physical interaction with $\alpha 2\delta$-1 for surface and synaptic trafficking (J. Chen et al., 2018; M. H. Zhou et al., 2021b).

mGluR5 and NMDARs at primary afferent central terminals likely contribute, in a reciprocal fashion, to opioid-induced potentiation of glutamatergic input to spinal dorsal horn neurons. mGluR5 activation increases the activity and phosphorylation of NMDARs in the brain (Choe et al., 2006; D. P. Li et al., 2014). Increased PKC activity is probably involved in the mGluR5–NMDAR interaction potentiated by opioids. In this regard, brief opioid exposure triggers NMDAR-mediated LTP via PKC (S. R. Chen et al., 2022). Increased PKC activity plays a major role in opioid-induced presynaptic NMDAR hyperactivity in the spinal cord and hyperalgesia (Mao et al., 1994; Zhao et al., 2012; S. R. Chen et al., 2022). Also, PKC binds to and acts on both mGluR5 and NMDARs (J. H. Lee et al., 2008; M. H. Zhou et al., 2021b). In addition, increased mGluR5 activity by opioid treatment may increase Gαq/11 availability, thereby increasing NMDAR activity via PKC-mediated NMDAR phosphorylation in the spinal dorsal horn. A recent study indicates that Gαq is required for PKC activation by Gαi/o-coupled receptors (Pfeil et al., 2020). Therefore, mGluR5 could potentiate and/or maintain NMDAR phosphorylation and activity via the canonical Gαq/11-coupled PLC/PKC signaling cascade. On the other hand, opioid-induced presynaptic NMDAR hyperactivity causes excess glutamate release, which can induce sustained activation of mGluR5 at primary afferent central terminals.

In conclusion, our findings provide new evidence linking presynaptic mGluR5 to opioid-induced NMDAR hyperactivity in the spinal cord and the resulting hyperalgesia and tolerance (Fig. 9). The two distinct glutamate receptors at primary afferent central terminals dynamically interact to facilitate the development of opioid-induced hyperalgesia and tolerance. This information not only extends our mechanistic understanding of how mGluR5 and NMDARs are mutually involved in opioid-induced hyperalgesia and tolerance but also suggests new targets for treating this condition. Inhibiting mGluR5 activity or disrupting the mGluR5–NMDAR interaction may be effective for treating patients with opioid use disorder and improving opioids' efficacy for pain control.

References

Abdul-Ghani MA, Valiante TA, Carlen PL, Pennefather PS (1996) Metabotropic glutamate receptors coupled to IP3 production mediate inhibition of IAHP in rat dentate granule neurons. J Neurophysiol 76:2691–2700.

Alvarez FJ, Villalba RM, Carr PA, Grandes P, Somohano PM (2000) Differential distribution of metabotropic glutamate receptors 1a, 1b, and 5 in the rat spinal cord. J Comp Neurol 422:464–487.

Aronica E, Catania MV, Geurts J, Yankaya B, Troost D (2001) Immunohistochemical localization of group I and II metabotropic glutamate receptors in control and amyotrophic lateral sclerosis human spinal cord: upregulation in reactive astrocytes. Neuroscience 105:509–520.

Bhave G, Nadin BM, Brasier DJ, Glauner KS, Shah RD, Heinemann SF, Karim F, Gereau RW (2003) Membrane topology of a metabotropic glutamate receptor. J Biol Chem 278:30294–30301.

Bodzęta A, Scheefhals N, MacGillavry HD (2021) Membrane trafficking and positioning of mGluRs at presynaptic and postsynaptic sites of excitatory synapses. Neuropharmacology 200:108799.

Cai YQ, Chen SR, Han HD, Sood AK, Lopez-Berestein G, Pan HL (2009) Role of M2, M3, and M4 muscarinic receptor subtypes in the spinal cholinergic control of nociception revealed using siRNA in rats. J Neurochem 111:1000–1010.

Chaplan SR, Bach FW, Pogrel JW, Chung JM, Yaksh TL (1994) Quantitative assessment of tactile allodynia in the rat paw. J Neurosci Methods 53:55–63.

Chen J, Li L, Chen SR, Chen H, Xie JD, Sirrieh RE, MacLean DM, Zhang Y, Zhou MH, Jayaraman V, Pan HL (2018) The $\alpha 2\delta$-1-NMDA receptor complex is critically involved in neuropathic pain development and gabapentin therapeutic actions. Cell Rep 22:2307–2321.

Chen SR, Pan HL (2006) Loss of TRPV1-expressing sensory neurons reduces spinal mu opioid receptors but paradoxically potentiates opioid analgesia. J Neurophysiol 95:3086–3096.

Chen SR, Prunean A, Pan HM, Welker KL, Pan HL (2007) Resistance to morphine analgesic tolerance in rats with deleted transient receptor potential vanilloid type 1-expressing sensory neurons. Neuroscience 145:676–685.

Chen SR, Hu YM, Chen H, Pan HL (2014a) Calcineurin inhibitor induces pain hypersensitivity by potentiating pre- and postsynaptic NMDA receptor activity in spinal cords. J Physiol 592:215–227.

Chen SR, Zhu L, Chen H, Wen L, Laumet G, Pan HL (2014b) Increased spinal cord Na^+-K^+-$2Cl^-$ cotransporter-1 (NKCC1) activity contributes to impairment of synaptic inhibition in paclitaxel-induced neuropathic pain. J Biol Chem 289:31111–31120.

Chen SR, Chen H, Jin D, Pan HL (2022) Brief opioid exposure paradoxically augments primary afferent input to spinal excitatory neurons via $\alpha 2\delta$-1-dependent presynaptic NMDA receptors. J Neurosci 42:9315–9329.

Chen Y, Chen SR, Chen H, Zhang J, Pan HL (2019) Increased $\alpha 2\delta$-1-NMDA receptor coupling potentiates glutamatergic input to spinal dorsal horn neurons in chemotherapy-induced neuropathic pain. J Neurochem 148:252–274.

Choe ES, Shin EH, Wang JQ (2006) Regulation of phosphorylation of NMDA receptor NR1 subunits in the rat neostriatum by group I metabotropic glutamate receptors in vivo. Neurosci Lett 394:246–251.

Conn PJ, Pin JP (1997) Pharmacology and functions of metabotropic glutamate receptors. Annu Rev Pharmacol Toxicol 37:205–237.

Copani A, Romano C, Di Giorgi Gerevini V, Nicosia A, Casabona G, Storto M, Mutel V, Nicoletti F (2000) Reducing conditions differentially affect the functional and structural properties of group-I and -II metabotropic glutamate receptors. Brain Res 867:165–172.

da Silva S, Hasegawa H, Scott A, Zhou X, Wagner AK, Han BX, Wang F (2011) Proper formation of whisker barrelettes requires periphery-derived Smad4-dependent TGF-beta signaling. Proc Natl Acad Sci USA 108:3395–3400.

Deng M, Chen SR, Chen H, Pan HL (2019a) $\alpha 2\delta$-1-bound N-methyl-D-aspartate receptors mediate morphine-induced hyperalgesia and analgesic tolerance by potentiating glutamatergic input in rodents. Anesthesiology 130:804–819.

Deng M, Chen SR, Chen H, Luo Y, Dong Y, Pan HL (2019b) Mitogen-activated protein kinase signaling mediates opioid-induced presynaptic NMDA receptor activation and analgesic tolerance. J Neurochem 148:275–290.

El Moustaine D, Granier S, Doumazane E, Scholler P, Rahmeh R, Bron P, Mouillac B, Baneres JL, Rondard P, Pin JP (2012) Distinct roles of metabotropic glutamate receptor dimerization in agonist activation and G-protein coupling. Proc Natl Acad Sci USA 109:16342–16347.

Finnegan TF, Li DP, Chen SR, Pan HL (2004) Activation of mu-opioid receptors inhibits synaptic inputs to spinally projecting rostral ventromedial medulla neurons. J Pharmacol Exp Ther 309:476–483.

Hermans E, Challiss RA (2001) Structural, signalling and regulatory properties of the group I metabotropic glutamate receptors: prototypic family C G-protein-coupled receptors. Biochem J 359:465–484.

Higerd-Rusli GP, Tyagi S, Liu S, Dib-Hajj FB, Waxman SG, Dib-Hajj SD (2023) The fates of internalized Na(V)1.7 channels in sensory neurons: retrograde cotransport with other ion channels, axon-specific recycling, and degradation. J Biol Chem 299:102816.

Huang M, Luo L, Zhang Y, Wang W, Dong J, Du W, Jiang W, Xu T (2019) Metabotropic glutamate receptor 5 signalling induced NMDA receptor subunits alterations during the development of morphine-induced antinociceptive tolerance in mouse cortex. Biomed Pharmacother 110:717–726.

Huang Y, Chen SR, Chen H, Luo Y, Pan HL (2020) Calcineurin inhibition causes $\alpha2\delta$-1-mediated tonic activation of synaptic NMDA receptors and pain hypersensitivity. J Neurosci 40:3707–3719.

Huang Y, Chen SR, Chen H, Zhou JJ, Jin D, Pan HL (2022) Theta-burst stimulation of primary afferents drives long-term potentiation in the spinal cord and persistent pain via $\alpha2\delta$-1-bound NMDA receptors. J Neurosci 42:513–527.

Huang Y, Chen H, Jin D, Chen SR, Pan HL (2023) NMDA receptors at primary afferent-excitatory neuron synapses differentially sustain chemotherapy- and nerve trauma-induced chronic pain. J Neurosci 43:3933–3948.

Hudson LJ, Bevan S, McNair K, Gentry C, Fox A, Kuhn R, Winter J (2002) Metabotropic glutamate receptor 5 upregulation in A-fibers after spinal nerve injury: 2-methyl-6-(phenylethynyl)-pyridine (MPEP) reverses the induced thermal hyperalgesia. J Neurosci 22:2660–2668.

Hunter DV, Smaila BD, Lopes DM, Takatoh J, Denk F, Ramer MS (2018) Advillin is expressed in all adult neural crest-derived neurons. eNeuro 5: ENEURO.0077-18.2018.

Jin D, Chen H, Huang Y, Chen SR, Pan HL (2022) δ-Opioid receptors in primary sensory neurons tonically restrain nociceptive input in chronic pain but do not enhance morphine analgesic tolerance. Neuropharmacology 217:109202.

Kim YH, Park CK, Back SK, Lee CJ, Hwang SJ, Bae YC, Na HS, Kim JS, Jung SJ, Oh SB (2009) Membrane-delimited coupling of TRPV1 and mGluR5 on presynaptic terminals of nociceptive neurons. J Neurosci 29:10000–10009.

Ko SJ, Isozaki K, Kim I, Lee JH, Cho HJ, Sohn SY, Oh SR, Park S, Kim DG, Kim CH, Roche KW (2012) PKC phosphorylation regulates mGluR5 trafficking by enhancing binding of Siah-1A. J Neurosci 32:16391–16401.

Lee J, Munguba H, Gutzeit VA, Singh DR, Kristt M, Dittman JS, Levitz J (2020) Defining the homo- and heterodimerization propensities of metabotropic glutamate receptors. Cell Rep 31:107891.

Lee JH, Lee J, Choi KY, Hepp R, Lee JY, Lim MK, Chatani-Hinze M, Roche PA, Kim DG, Ahn YS, Kim CH, Roche KW (2008) Calmodulin dynamically regulates the trafficking of the metabotropic glutamate receptor mGluR5. Proc Natl Acad Sci USA 105:12575–12580.

Li DP, Zhu LH, Pachuau J, Lee HA, Pan HL (2014) mGluR5 Upregulation increases excitability of hypothalamic presympathetic neurons through NMDA receptor trafficking in spontaneously hypertensive rats. J Neurosci 34:4309–4317.

Li JQ, Chen SR, Chen H, Cai YQ, Pan HL (2010) Regulation of increased glutamatergic input to spinal dorsal horn neurons by mGluR5 in diabetic neuropathic pain. J Neurochem 112:162–172.

Li L, Chen SR, Chen H, Wen L, Hittelman WN, Xie JD, Pan HL (2016) Chloride homeostasis critically regulates synaptic NMDA receptor activity in neuropathic pain. Cell Rep 15:1376–1383.

Liu JB, Yao YX, Jiang W (2009) Inhibitory effects of Group I metabotropic glutamate receptors antagonists on the expression of NMDA receptor NR1 subunit in morphine tolerant rats. Neurosci Lett 452:268–272.

Mao J, Price DD, Mayer DJ (1994) Thermal hyperalgesia in association with the development of morphine tolerance in rats: roles of excitatory amino acid receptors and protein kinase C. J Neurosci 14:2301–2312.

Mao L, Wang JQ (2002) Interactions between ionotropic and metabotropic glutamate receptors regulate cAMP response element-binding protein phosphorylation in cultured striatal neurons. Neuroscience 115:395–402.

Marwari S, Kowalski C, Martemyanov KA (2022) Exploring pharmacological inhibition of G(q/11) as an analgesic strategy. Br J Pharmacol 179:5196–5208.

Miura M, Watanabe M, Offermanns S, Simon MI, Kano M (2002) Group I metabotropic glutamate receptor signaling via Galpha q/Galpha 11 secures the induction of long-term potentiation in the hippocampal area CA1. J Neurosci 22:8379–8390.

Narita M, Suzuki M, Narita M, Niikura K, Nakamura A, Miyatake M, Aoki T, Yajima Y, Suzuki T (2005) Involvement of spinal metabotropic glutamate receptor 5 in the development of tolerance to morphine-induced antinociception. J Neurochem 94:1297–1305.

Ojha P, Pal S, Bhattacharyya S (2022) Regulation of metabotropic glutamate receptor internalization and synaptic AMPA receptor endocytosis by the postsynaptic protein norbin. J Neurosci 42:731–748.

Palczewski K (2010) Oligomeric forms of G protein-coupled receptors (GPCRs). Trends Biochem Sci 35:595–600.

Pfeil EM, et al. (2020) Heterotrimeric G protein subunit Galphaq is a master switch for Gbetagamma-mediated calcium mobilization by Gi-coupled GPCRs. Mol Cell 80:940–954.e946.

Romano C, Yang WL, O'Malley KL (1996) Metabotropic glutamate receptor 5 is a disulfide-linked dimer. J Biol Chem 271:28612–28616.

Sanjana NE, Shalem O, Zhang F (2014) Improved vectors and genome-wide libraries for CRISPR screening. Nat Methods 11:783–784.

Scheefhals N, Westra M, MacGillavry HD (2023) mGluR5 is transiently confined in perisynaptic nanodomains to shape synaptic function. Nat Commun 14:244.

Schroder H, Wu DF, Seifert A, Rankovic M, Schulz S, Hollt V, Koch T (2009) Allosteric modulation of metabotropic glutamate receptor 5 affects phosphorylation, internalization, and desensitization of the micro-opioid receptor. Neuropharmacology 56:768–778.

Shalem O, Sanjana NE, Hartenian E, Shi X, Scott DA, Mikkelson T, Heckl D, Ebert BL, Root DE, Doench JG, Zhang F (2014) Genome-scale CRISPR-Cas9 knockout screening in human cells. Science 343:84–87.

Sotgiu ML, Bellomi P, Biella GE (2003) The mGluR5 selective antagonist 6-methyl-2-(phenylethynyl)-pyridine reduces the spinal neuron pain-related activity in mononeuropathic rats. Neurosci Lett 342:85–88.

Sprengel R, Suchanek B, Amico C, Brusa R, Burnashev N, Rozov A, Hvalby O, Jensen V, Paulsen O, Andersen P, Kim JJ, Thompson RF, Sun W, Webster LC, Grant SG, Eilers J, Konnerth A, Li J, McNamara JO, Seeburg PH (1998) Importance of the intracellular domain of NR2 subunits for NMDA receptor function in vivo. Cell 92:279–289.

Sun J, Chen SR, Chen H, Pan HL (2019) μ-Opioid receptors in primary sensory neurons are essential for opioid analgesic effect on acute and inflammatory pain and opioid-induced hyperalgesia. J Physiol 597: 1661–1675.

Traynelis SF, Wollmuth LP, McBain CJ, Menniti FS, Vance KM, Ogden KK, Hansen KB, Yuan H, Myers SJ, Dingledine R (2010) Glutamate receptor ion channels: structure, regulation, and function. Pharmacol Rev 62:405–496.

Valerio A, Rizzonelli P, Paterlini M, Moretto G, Knopfel T, Kuhn R, Memo M, Spano P (1997) mGluR5 metabotropic glutamate receptor distribution in rat and human spinal cord: a developmental study. Neurosci Res 28:49–57.

Xie JD, Chen SR, Pan HL (2017) Presynaptic mGluR5 receptor controls glutamatergic input through protein kinase C-NMDA receptors in paclitaxel-induced neuropathic pain. J Biol Chem 292:20644–20654.

Xie JD, Chen SR, Chen H, Zeng WA, Pan HL (2016) Presynaptic N-methyl-D-aspartate (NMDA) receptor activity is increased through protein kinase C in paclitaxel-induced neuropathic pain. J Biol Chem 291:19364–19373.

Xie W, Samoriski GM, McLaughlin JP, Romoser VA, Smrcka A, Hinkle PM, Bidlack JM, Gross RA, Jiang H, Wu D (1999) Genetic alteration of phospholipase C beta3 expression modulates behavioral and cellular responses to mu opioids. Proc Natl Acad Sci USA 96:10385–10390.

Xu T, Jiang W, Du D, Xu Y, Hu Q, Shen Q (2007) Role of spinal metabotropic glutamate receptor subtype 5 in the development of tolerance to morphine-induced antinociception in rat. Neurosci Lett 420:155–159.

Yang L, Mao L, Tang Q, Samdani S, Liu Z, Wang JQ (2004) A novel Ca^{2+}-independent signaling pathway to extracellular signal-regulated protein kinase by coactivation of NMDA receptors and metabotropic glutamate receptor 5 in neurons. J Neurosci 24:10846–10857.

Zappia KJ, O'Hara CL, Moehring F, Kwan KY, Stucky CL (2017) Sensory neuron-specific deletion of TRPA1 results in mechanical cutaneous sensory deficits. eNeuro 4:ENEURO.0069-16.2017.

Zhang GF, Chen SR, Jin D, Huang Y, Chen H, Pan HL (2021) $\alpha 2\delta$-1 upregulation in primary sensory neurons promotes NMDA receptor-mediated glutamatergic input in resiniferatoxin-induced neuropathy. J Neurosci 41:5963–5978.

Zhang J, Chen SR, Zhou MH, Jin D, Chen H, Wang L, DePinho RA, Pan HL (2022) HDAC2 in primary sensory neurons constitutively restrains chronic pain by repressing $\alpha 2\delta$-1 expression and associated NMDA receptor activity. J Neurosci 42:8918–8935.

Zhao YL, Chen SR, Chen H, Pan HL (2012) Chronic opioid potentiates presynaptic but impairs postsynaptic N-methyl-D-aspartic acid receptor activity in spinal cords: implications for opioid hyperalgesia and tolerance. J Biol Chem 287:25073–25085.

Zhou HY, Chen SR, Chen H, Pan HL (2010) Opioid-induced long-term potentiation in the spinal cord is a presynaptic event. J Neurosci 30:4460–4466.

Zhou JJ, Pachuau J, Li DP, Chen SR, Pan HL (2020) Group III metabotropic glutamate receptors regulate hypothalamic presympathetic neurons through opposing presynaptic and postsynaptic actions in hypertension. Neuropharmacology 174:108159.

Zhou JJ, Shao JY, Chen SR, Li DP, Pan HL (2021a) $\alpha 2\delta$-1-dependent NMDA receptor activity in the hypothalamus is an effector of genetic-environment interactions that drive persistent hypertension. J Neurosci 41:6551–6563.

Zhou MH, Chen SR, Wang L, Huang Y, Deng M, Zhang J, Zhang J, Chen H, Yan J, Pan HL (2021b) Protein kinase C-mediated phosphorylation and $\alpha 2\delta$-1 interdependently regulate NMDA receptor trafficking and activity. J Neurosci 41:6415–6429.